

Surface Passivation at Cryogenic Temperatures

Furkan Kaya

Fall 2017
TFY4520 - Specialization project
Department of Physics
Norwegian University of Science and Technology, NTNU

Supervisor at NTNU: Jon Andreas Stovneng
Supervisors at JV and IFE: Jarle Gran and Halvard Haug



NTNU – Trondheim
Norwegian University of
Science and Technology

To my uncle Mehmed (Memo) Darez who passed away this year. May the infinite realm provide you a home worthy of your stature in the finite realm. Your soul will forever live through me!

Acknowledgments

This specialization project represents preparatory work for a master thesis in Nanotechnology at NTNU. Custom implies that the supervisors should get the first referral in an acknowledgement section. That tradition will be continued here as well. I still remember this summer when I first moved to the Kjeller area, without any master assignment and few contacts in the district. So therefore an initial mention has to be given to the person that introduced me to the science of photodiodes and gave me this assignment, Dr. Jarle Gran. Dr. Gran is considered the foremost expert on photodiodes in Norway. My gratitude to you for giving me this opportunity.

Next in line for my appreciations is my co-supervisor at IFE, Dr. Halvard Haug. Having seen an almost meteoric rise in the scientific world with an impressive foray of research, and still very young, I feel privileged to be able to work with Dr. Haug. Also special thanks to my supervisor at NTNU, Dr. Jon Andreas Stovneng, for taking me in at a crucial time. I am unsure if anyone else would've taken this task, but Dr. Stovneng did.

A person that did not have any formal role in forming my work, but had an elevated influence due to him always being available for any questions, was Dr. Chi Kwong Tang. Dr. Tang's ideas and intelligent thoughts on various issues made him an influential figure in this work. A warm thank you to Dr. Tine Uberg Nærland for giving me help in designing the measurement stage for QssPC.

I must honestly admit that I never thought I would get this far. With almost going blind on four different instances with three eye diseases and sometimes going to exams either partly or entirely blind, it must be almost be considered a modern miracle that I am on the verge of writing a master thesis. But the credit is not mine alone, special thanks have to be given to my father for financing my education both here and back when I studied history, economics and political science. During my illness my much beloved mother functioned as not only my mother, but also my nurse. I will forever be grateful for the moral you imprinted into me from childhood and into adult age. Also special considerations are given to my two sisters, who have given me a window into the life outside science and politics.

Summary

A new detector based on the principle of photodiode has been developed by Justervesenet (Norwegian Metrology Service). The Predictable Quantum Efficient Detector with the acronyms PQED has gone through extensive simulations. Those indicated that a considerable improvement in lifetime is expected at 77 K compared to 298 K. Reason for this is a decreasing surface recombination by a logarithmic factor of 1 to 2.

Two measurement stages were developed and tested for use at 77 K. The stages were created for QssPC and PL tools due to their fragility and high cost. Several experiments were done and their proceedings are walked through step by step, before the entire process is evaluated according to predetermined criteria.

Results from the cryogenic experiments showed a significant decrease in lifetime for all the six samples measured on in this project. The samples had different passivation layers, some had purely nitride with a variation in refractive indexes and others had a combination of nitride, oxide and hydrogen (also referred to as oxynitrides) passivation layers. Some difference between nitride and oxynitride layers were seen, but intra-differences were more pronounced. Theories for why this phenomena occurred is given and both refractive indexes and gas level deposition are mentioned in this regard.

Several experiments were conducted at high (HT) and room temperatures (RT) in order to provide comparisons to the measurements done at cryogenic temperatures (CT). The experiments indicated that the tendency seen at CT conditions were continued at higher temperatures. A side-effect of these experiments is that a correction for mobility is also included in the text.

I-V measurements were done at Justervesenet for measuring the linearity and IQD for actual photodiodes at both room and cryogenic temperature. These measurements were used to investigate how the diodes behaved in those extreme conditions and for providing a background for why there was some discrepancy between those measurements and the lifetime measurements. The IQD decreased for the diodes, but did not do so for the Silicon-wafer samples.

Finally, the measurement stage for Photoluminescence-Imaging was tried out. The results from the experiment confirmed the decreasing lifetimes, but photoluminescence is largely based on radiative recombination. In the indirect semiconductor material that is Silicon, radiative recombination is not as influential. However, the measurement stage worked and the results from the experiment could be used to find the level of other recombinations.

Table of Contents

Acknowledgements	i
Summary	ii
Table of Contents	iv
List of Tables	v
List of Figures	viii
Abbreviations	ix
1 Introduction	1
1.1 Goals with the assignment	2
1.2 Outline	2
2 Photodiode theory	5
2.1 PN junction Photodiode	5
2.1.1 Induced Photodiode	6
2.1.2 The inner photoelectric effect	8
2.1.3 Operation of Photodiodes	9
2.1.4 Dark current	9
2.1.5 Responsivity	10
2.1.6 Internal quantum deficiency	10
2.1.7 Uncertainty of Photodiodes	11
2.2 Comparative simulations from JV	11
2.3 Cooling of diodes	15
3 Photodiode experiments and results	17
3.1 I-V measurements at Justervesenet	17
3.1.1 Laser setup at JV	18
3.2 I-V experiment	18

3.3	Results	19
3.4	Summary of the I-V measurement results	22
3.5	Relationship between I-V experiments and recombination experiments	23
4	Recombination and characterization theory	25
4.1	Lifetime of carriers	25
4.1.1	Bulk recombination	26
4.1.2	Surface recombination	27
4.2	Passivation and materials	30
4.2.1	Surface passivation - background	30
4.2.2	SiO ₂ passivation	30
4.2.3	SiN _x passivation	30
4.3	QssPC for lifetime measurements	31
4.4	QssPC measurement stage	32
4.5	PL Imaging for lifetime measurements	34
4.6	PL measurement stage	35
4.7	The samples	36
5	Recombination experiments and results	39
5.1	The QssPC experiment	39
5.2	QssPC results and discussion	40
5.2.1	Coil and temperature influence	40
5.2.2	Sample lifetime measurements	40
5.2.3	Explaining the lifetime values	43
5.2.4	Mobility approximation	45
5.2.5	High temperature measurement experiment for comparison	46
5.2.6	Evaluation of the measurement stage	49
5.3	PL experiment	50
5.4	PL results and discussion	51
5.4.1	Evaluation of the measurement stage	54
6	Overview of the results	57
7	Conclusion	59
7.1	Possible future work	59
Appendix		63

List of Tables

2.1	Table over simulated IQD. It should be pointed out that all the results are predictions	13
2.2	The default simulation parameters in the simulation, e symbolizes the potency 10.[1]	14
3.1	Table shows the input parameters for the experiment conducted at JV	20
4.1	Table over the samples with sample name, passivation layer and PECVD parameters	36
5.1	Table shows the sample numbers, temperature and lifetimes at respectively RT and CT	43
5.2	Table shows the relationship between E_t , k and lifetime. R. in column is recombination	44

List of Figures

2.1	Schematic drawing and band structure of a p-n junction. In equilibrium, diffusion and drift currents balance each other.[2]	6
2.2	Schematic of induced junction detector (Front passivation layer in blue).[3]	7
2.3	Charges and their location for thermally oxidized silicon. The charges are as following, based on numeration: (1) Interface trapped charge, (2) Fixed oxide charge, (3) Oxide trapped charge, (4) Mobile oxide charge.[4]	7
2.4	Current-voltage characteristic of a photodiode with and without illumination. Different sections of the curve correspond to different modes of reading out the signal To the right is a diode equivalent circuit inserted.[2]	9
2.5	Simulated Internal quantum deficiency as a function wavelength for different SRV parameters. Image provided at the courtesy of Chi Kwong Tang.	12
2.6	Schematic of how the induced junction diode on figure 2.2 is designed in Cogenda Genius. Schematic provided at the courtesy of Chi Kwong Tang	13
2.7	Schematic of IQD as a function of wavelength for both CT and RT conditions. Red color indicates CT and green RT. Figure provided at the courtesy of Chi Kwong Tang	15
3.1	Schematic of the circuit used in the JV laboratory	18
3.2	Picture montage of the laser setup at JV. (I) Optics to clean and align the laser. A shutter and a power stabilizer is visible near the bottom of the picture. (II) Cryostat with the detector inside.	19
3.3	I-V curve with the parameters and $1500 \mu\text{W}$ in optical power as given and with blue line = CT and red line = RT, since they traditionally symbolizes those colours.	20
3.4	Schematic of the type A uncertainty as a function of voltage for both cryogenic and room temperature. Red = RT and blue = CT	21
3.5	Schematic of the relative uncertainty for CT=blue and RT=red. X and y-axis lack axis-labels due to overprocessing in the Excel-file. X-axis = voltage and y-axis = IQD.	22

4.1	Recombination mechanisms:(a) SRH, (b) radiative, and (c) Auger.[4]	26
4.2	Band diagram of the (p-type) silicon surface under non-equilibrium conditions, and with non-zero surface band-bending (accumulation), showing definitions of relevant energies and potentials.[5]	29
4.3	An image of the WCT-120 instrument used for QssPC measurements.[6]	31
4.4	Picture montage of the entire process from calibration to measuring under CT conditions: (I) shows the setup with a circle that indicates sensors location. (II) the same setup from afar. (III) the calibration with the reference wafer. (IV) equipment used to transfer the LN2 and the container for freezing the temperature. (V) Pyrex petridish with wafer and LN2. (VI) Pyrex petridish placed on the WCT-120	33
4.5	Illustration of the PL imaging equipment. A defocused diode laser is used to inject carriers homogeneously over the wafer. The emitted PL light is then detected by a Si CCD camera, with a resolution down to $23 \mu m$.[7]	34
4.6	Picture montage of the PL-I measurement stage, from free standing to inserted in the PL equipment. (I) The isopore-box free standing. (II) The polished sample holder on top of the box. (III) The same sample holder viewed from the side. (IV) Cover of the box lifted up high in order to see how the Al-rod goes down to the bottom of the box. (V) A leveller is used to correct the upper position of the box, for more info referred to the experiment part. (VI) The box inserted into the PL equipment and both laser (with the danger signs attached to it on the right) and CCD camera (straight above the box) can be seen in this picture	37
5.1	Schematic of Sample 1 lifetime measurement vs time	40
5.2	Schematic of SiN_x passivated samples lifetime measurements vs time	41
5.3	Schematic of oxynitride passivated samples lifetime measurements vs time	42
5.4	Schematic of effective lifetime vs minority carrier density for different temperatures. The measured sample is Sample 2.	47
5.5	Schematic of effective lifetime vs minority carrier density for different temperatures. The measured sample is Sample 5.	48
5.6	Schematic of log/log scale plot of lifetime measurement vs minority carrier density for Sample 2 for HT, RT and CT. Lifetime is given in μs and minority carrier density in cm^{-3}	49
5.7	Images that shows the results obtained by PL-I for the SiN_x passivated layers. The upper image depicts Sample 2, the mid-tier image depicts Sample 3, while the last image depicts Sample 4. On all the rows, RT to the left and CT to the right	52
5.8	Images that show the results obtained by PL-I for the oxynitride passivated layer. The upper image depicts Sample 5 and the lower image depicts the Sample 6	53

Abbreviations

Al	=	Aluminum
C	=	Celsius
CT	=	Cryogenic temperature
c-Si	=	Crystalline Silicon
EHP	=	Electron-Hole pair
G	=	Generation
g	=	Conductance
HT	=	High temperature
IFE	=	Institute for Energy Technology
I-V	=	Current-Voltage
IQD	=	Internal Quantum Deficiency
JV	=	Justervesenet
K	=	Kelvin
kT	=	Thermal energy
LN2	=	Liquid Nitrogen
nm	=	nanometer
NTNU	=	Norwegian University of Science and Technology
PECVD	=	Plasma Enhanced Chemical Vapor Deposition
PL	=	Photoluminescence
PL-I	=	Photoluminescence Imaging
PL-V	=	Photoluminescence Imaging under applied bias
ppm	=	parts per million
PQED	=	Predictable Quantum Efficient Detector
QssPC	=	Quasi-Steady-State Photoconductance
RT	=	Room temperature
R	=	Recombination
s	=	seconds
sccm	=	standard cubic centimeter per minute
Si	=	Silicon
SRH	=	Shockley-Read-Hall
SRV	=	Surface Recombination Velocity

Introduction

The photodiode is a widely used semiconductor device that transforms incident optical power into electrical current. The responsivity of photodiodes can be estimated from fundamental constants, the wavelength of the radiation, the reflectance and internal losses of the photodiodes. Different variations and improvements of the photodiode exists and the Justervesenet (JV) has developed new Predictable Quantum Efficient Detector (PQED) photodiodes. The PQED is a new primary standard of optical power. The optical power is the energy per unit time. A critical parameter in judging the quality of a detector is the internal quantum deficiency (IQD). IQD is important in deciding the quality of photodiodes. The estimated uncertainty of IQD defines the achievable uncertainty in the response of the diode. Suggested uncertainty for the PQED at 1ppm could potentially give a new primary standard of optical power.

Based on simulations done by JV, the responsivity of the photodiode could be improved by one to two orders of magnitude at cryogenic temperatures. In this project an attempt has been made to cool diodes down to 77 K and to evaluate them separately and by changing the passivation layer for comparative reasons. In general, thin films like SiO_2 and SiN_x are used to reduce surface recombination and it is therefore imperative to investigate the defect states at these surfaces with changing temperature. This could lead to unprecedented accuracy and much improved detectors.

The simulations assumed that the surface recombination velocities (SRV) and bulk lifetime are the same at both room temperature (RT) and cryogenic temperature (CT). It showed that surface recombination (SRV) limits the achievable responsivity. Inferred from that, is the usefulness of lifetime measurements as a tool in characterization of SRV. In order to design the optimal diode for low temperatures, a characterization of SRV could give valuable information regarding expected behaviour from the diode at low temperatures and it would give the opportunity to apply different passivation materials for comparative reasons. From the experiments the optimal material could be picked out to create the optimal diode for low temperature.

Main intention of the assignment is to design a measurement stage, create the stage, adjust the parameters for the experiment for it to succeed and provide an evaluation of the results obtained from the experiments. Two measurement stages for the Quasi Steady State Photoconductance (QssPC) and Photoluminescence Imaging (PL-I) tools respectively are developed. High cost of equipment and fragility of the tools makes a measurement stage mandatory for these kind of experiments.

Additional experiments at higher temperatures, and experiments on a variation of samples have been done in order for creating cases of comparative results. Other aspects like developing a new mobility model more adjusted to CT measurements, rather than the existing models for RT and above, and ample scientific explanations for the measurements acquired from the novel experiments are done for future research within the field.

Furthermore, tests done at the JV were conducted on actual photodiodes. These test give a crucial connection between the photodiodes and the lifetime measurements done to improve those diodes. The results from I-V measurements could elaborate on how much improvement is needed for the photodiodes or whether there is some discrepancy between the results obtained at CT for the photodiodes and lifetime measurements.

1.1 Goals with the assignment

At the beginning of the project, based on previous works and theoretical ambidexterity of the subject, the assignment could go in many directions. A decision was made to limit the research to:

- Creating a measurement stage for measurements done under cryogenic conditions
- Material research enabling possibility to creating a potentially new standard of optical power based on fundamental constants by lowering IQD to below 1 ppm
- Development of methods for work at CT environment conditions and providing explanations on phenomena seen during this novel new research.
- Conducting tests on photodiodes at JV for measuring linearity and IQD

1.2 Outline

Chapter 2 gives the theoretical background for photodiodes, induced photodiodes, how diodes are affected by cooling, and an insight into the simulations done on photodiodes at JV.

Chapter 3 is about the experiments done on actual photodiode and the I-V measurements conducted. In this chapter the results acquired from these experiments are presented.

Chapter 4 elaborates on the experimental techniques that were used to investigate the SRV.

Different methods are used to measure the lifetimes. Two of them are QssPC and PL. Both techniques are available at IFE and two different measurement stages for CT conditions have been developed. These novel measurement stages developed are introduced in Chapter 4. Also available is the theoretical background for recombination and the tools used in the project.

Chapter 5 summarizes the results from the different experimental techniques done for lifetime measurements. The measurement stages are shown to function and the results are a consequence of that. It is sectioned according to the layout of chapter 4. Chapter 5 is the chapter where a thorough discussion is done regarding whether the goals outlined in the last section are met. Also in this chapter: a comprehensive evaluation of the results obtained.

Chapter 6 is an overview of all the results obtained by the different experiments. The intention of this chapter is to make it easier for the reader to evaluate the progress done in this project.

Chapter 7 shows the conclusion. A future work on both the measurement stages and passivation layers is included.

Chapter 2

Photodiode theory

Much of the work done in this project is founded in the intention on improving the photodiode. A basic introduction of a photodiode is done in this chapter.

The popularity of the photodiode is due to its simple and low cost nature. As a semiconductor device with two modes: photovoltaic (zero bias or forward bias voltage) and photoconductive (zero or reverse bias voltage), a wide range of applications are available for the photodiode. It is also very effective and can achieve high speed in electronics. For those reasons it is a widely used component that needs further improvements to keep in touch with the rest of the electronics field.

Photodiodes are used as a transfer standard at JV. A transfer standard is a standard used to calibrate other instruments. There is a main standard, often very valuable and should be used with extreme care, that calibrates a second instrument, called the working standard. The working standard is less valuable, but has higher uncertainty. This second instrument is referred to as the transfer standard and is used to calibrate other instruments. It has little loss, but needs calibration. JV has developed methods that can decide the losses directly and thereby make it a primary standard.

2.1 PN junction Photodiode

In instances where one dopes a semiconductor material like Silicon (Si) with a dopant like Boron (called an acceptor) or Phosphorous (called a donor), the product becomes a p-type or an n-type semiconductor. The terms n-type and p-type indicate whether an electron or a hole is majority carrier in that region. By joining together two pieces of semiconductor, n-type and p-type, a pn junction is formed in their interface. In the material near the junction, it is so that electrons will diffuse through the junction from the n-side to the p-side to combine with holes there, and opposite flow for holes in the p-side. This is called a diode. A photodiode is based on a pn junction in reverse bias voltage.[2] Its main function is to convert light into either current or voltage.

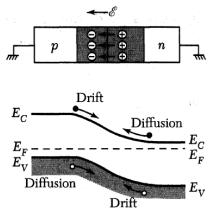


Figure 2.1: Schematic drawing and band structure of a p-n junction. In equilibrium, diffusion and drift currents balance each other.[2]

Electrical charge increases until an equilibrium is reached. At that state, the donor atoms will repel holes and acceptor atoms will repel electrons. The equilibrium gives origin to a potential barrier around the junction, as seen on figure 2.1 (upper part).

In the potential barrier, no free charge carriers exists. This creates a depletion layer in the proximity of the pn junction. A reverse bias increases the barrier and a consequence of that is that the subsequent decreasing of the majority carriers leads to the vanishing of them, while the drift current is the same.[9] But it also creates a situation with a small electric current. In order to increase this, more minority carriers have to generated. One way of doing this is by supplying external energy to the depletion layer. A photodiode is basically a diode where photons are as the external energy used to generate charge carriers in the depletion layer.

Absorption of the photons occur at the entire structure of the photodiode. However, the absorption at the depletion layer is responsible for the contribution to the current. An important parameter in this regard is the width of the depletion layer. This parameter gives the amount of area that absorbs the photons and is given by:

$$d = \sqrt{\frac{2\epsilon V_0}{q} \left(\frac{1}{n_d} + \frac{1}{n_a} \right)} \quad (2.1)$$

where q = charge of carrier, ϵ = permittivity, V_0 = the built-in voltage, and finally n_d and n_a are the doping levels for donors and acceptors.

2.1.1 Induced Photodiode

The induced junction photodiode structure was proposed and realised by T. Hansen in 1978.[10] Fixed positive surface state charge Q_{ss} inherent to thermally oxidized Si in-

The n-type and p-type semiconductors are separately electrically neutral. But joined together they form a pn junction. At the initial time of the fusion, some free electrons diffuse from the n-type material to the p-type in order to fill up the holes.[8] Positively charged donor ions are left behind because of this movement. As a result of that holes from the acceptor material move across the junction in the other direction.

Diffusion like from the paragraph above gives a positive charge density at the n-type material and a negative charge density at the p-type. The electrical charge increases until an equilibrium is reached. At that state, the donor atoms will repel holes and acceptor atoms will repel electrons. The equilibrium gives origin to a potential barrier around the junction, as seen on figure 2.1 (upper part).

In the potential barrier, no free charge carriers exists. This creates a depletion layer in the proximity of the pn junction. A reverse bias increases the barrier and a consequence of that is that the subsequent decreasing of the majority carriers leads to the vanishing of them, while the drift current is the same.[9] But it also creates a situation with a small electric current. In order to increase this, more minority carriers have to generated. One way of doing this is by supplying external energy to the depletion layer. A photodiode is basically a diode where photons are as the external energy used to generate charge carriers in the depletion layer.

Absorption of the photons occur at the entire structure of the photodiode. However, the absorption at the depletion layer is responsible for the contribution to the current. An important parameter in this regard is the width of the depletion layer. This parameter gives the amount of area that absorbs the photons and is given by:

$$d = \sqrt{\frac{2\epsilon V_0}{q} \left(\frac{1}{n_d} + \frac{1}{n_a} \right)} \quad (2.1)$$

where q = charge of carrier, ϵ = permittivity, V_0 = the built-in voltage, and finally n_d and n_a are the doping levels for donors and acceptors.

duces a n-type inversion layer on lightly-doped p-type materials. From this a shallow pn junction is formed. No diffusion process is needed. On figure 2.2, the PQED photodiode based on induced junction developed by JV and several European collaborators can be seen.

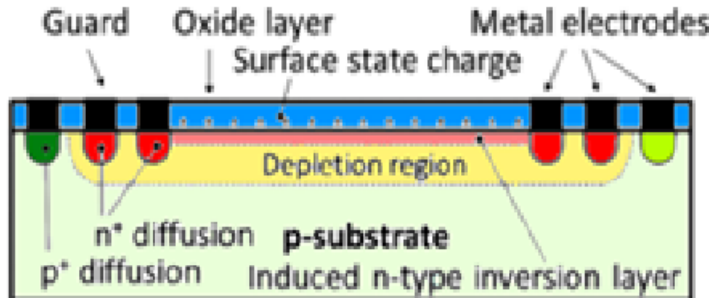


Figure 2.2: Schematic of induced junction detector (Front passivation layer in blue).[3]

It has a low doping concentration of $2 \times 10^{12} \text{ cm}^{-3}$ on a p-type Si.[11] On top of it an oxide layer smaller than 200 nm is added. The thermally grown thick oxide layer contains trapped surface charge in the proximity to the Si-SiO₂ boundary.[3] n⁺-diffusion rings functions as contacting for the inversion layer. The p⁺ serves as guarding and terminated the inversion layer.[10] A simple structure is the main factor in attributing the device as predictable.

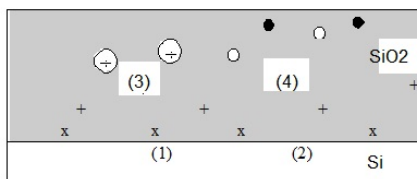


Figure 2.3: Charges and their location for thermally oxidized silicon. The charges are as following, based on numeration: (1) Interface trapped charge, (2) Fixed oxide charge, (3) Oxide trapped charge, (4) Mobile oxide charge.[4]

With the SiO₂ layer deposited on top of Si, there are four types of oxide charges: fixed oxide charge, interface trapped charge, mobile oxide charge and oxide trapped charge. They all contribute to the total charge of the system.[4]

(1) in figure 2.3 are positive or negative charges due to defects and located at the interface. It is also in electrical contact with the Si beneath it. (2) is a positive charge near the interface related to the oxidation process and therefore dependent on parameters like temperature and cooling conditions. Not in electrical contact with the Si. (3) can be positive or negative and is generated due to the carriers trapped in the oxide.

Combined, these positive charges repel the positive holes in the wafer and create a depletion region close to the Si-SiO₂ interface. The region will be depleted of holes and

free electrons will likewise be attracted to the interface. An n-type inversion layer in the p-type is the result and creates the depletion region can be further extended to the bulk by applying a reverse bias. Effectively, this increases the collection efficiency of charge carriers.[3]

The silicon surface Q_{ss} induces the depletion layer charge Q_b and the charge Q_n in the inversion layer. Due to the finite widths of the depletion layer a charge Q_g will be induced on the outer surface charge. Charge neutrality required:

$$Q_{ss} + Q_b + Q_g + Q_n = 0 \quad (2.2)$$

For the Q_{ss} to produce the inversion, a condition must be fulfilled:

$$Q_{ss}(1 - \frac{d}{2x_0}) + Q_b(1 + \frac{\epsilon_{0x}x_{d,max}}{2\epsilon_dx_0}) \geq 0 \quad (2.3)$$

One important parameter is the thickness of the passivation layer deposited on Si. It gives the possibility to suppress specular (mirror-like) reflectance with a proper thickness. But the thickness can not be freely chosen due to the fact that the thickness of the layer gives the density of charge for inversion layer. A thicker oxide leads to an easier obtainable inversion layer.[3]

Different passivation materials are commonly used. And the theory applies for all materials, but their properties are different.

2.1.2 The inner photoelectric effect

A photodiode's working principle is based on photoelectric effect. The reasoning for the effect was given by Einstein in 1905 and this gave him the Nobel Prize in Physics. In explaining the effect it is common to point to an experiment where light is incident on a metal plate. The electrons in the metal absorb the energy from the light, and some of the electrons receive enough energy to exit from the surface of the metal.[12] Einstein suggested that the energy of the photon was decided by the frequency of the light by the equation: $E = hv$, with h being the Planck's constant and v as the frequency. This means that the electrons receive an energy of hv and lose an amount of energy referred to as w in escaping from the surface of the metal. Combining all that above gives us the equation for the photoelectric effect, K:

$$K = hv - w \quad (2.4)$$

where w is the work function for removing an electron from the metal and varies by the metal used.[13]

With regards to the photodiode, a closely related phenomena referred to as inner photoelectric effect is experienced. From semiconductor physics there is that a band gap is the difference between the lowest energy of the conduction band and the highest energy of the valence band.[14] The size of the band gap decides whether the material is a metal, semiconductor or insulator. When the temperature is increased the electrons are excited from

the valence band and into the conduction band. In the inner photoelectric effect the electrons receive the energy-increase from the absorbed photons and kicks to the conduction band. The size of the photon's energy must be larger than as the semiconductors bandgap.

2.1.3 Operation of Photodiodes

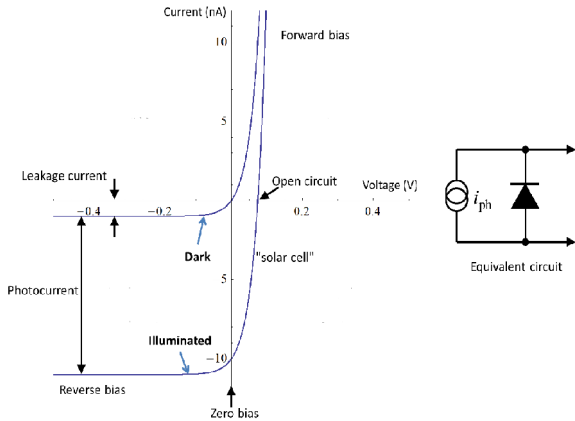


Figure 2.4: Current-voltage characteristic of a photodiode with and without illumination. Different sections of the curve correspond to different modes of reading out the signal To the right is a diode equivalent circuit inserted.[2]

According to figure 2.2, illumination changes the current-voltage characteristics of the diode.[2] Since there is reverse bias, the flow of current is largely dependent on illumination. The actual flow of current through the diode is given by the equation:

$$i = i_0(e^{\frac{qV}{kT}}) - i_{ph} \quad (2.5)$$

where V = applied voltage, k = Boltzmann's constant, T = temperature, i_{ph} = photogenerated current, i_0 = current in the non-illuminated diode.

It should also be mentioned that when a photodiode operates with a reverse bias, the photodiode becomes an ideal current source. Suggesting that if there is an external circuit attached to the diode, one could work on a principle of a 1:1 ratio between incident photons and ejected photoelectrons.[15] Due to the projects use of a Si-semiconductor with a bandgap of 1.1 eV, it becomes that the photodiode is sensitive to light between 200 nm and 1100 nm. Visible light has a spectral range between 400 and 700 nm.

2.1.4 Dark current

During a measurement where the current is assumed to be zero, but is not, a phenomena called for dark current has most likely occurred. The dark current is typically caused by

thermal excitation's of electrons in the detector.[2] Therefore, an integral part of laboratory work with diodes includes detection and counting the amount of dark current. This is done because dark current gives unwanted addition of photocurrent to the total photon count, based on the relation:

$$I_{total} = I_{ph} + I_{dark} \quad (2.6)$$

For a photodiode, one should remember that the diffusion current becomes minimal when a reverse bias is used, while the drift current is the same. For that reason it is considered that dark current is thermally generated minority carriers with concentration p_{n0} on the n-side.[2] Diffusion current is assumed to be the dominating form of dark current in the diode and based on the n-side alone (due to simplicity), to get the equation:

$$i_0 \approx q \frac{n_p D_e}{L_e} A_d \quad (2.7)$$

where n_p = minority carrier concentration, D_e = diffusion constant, L_e = diffusion length for electrons, A_d = area. The i_0 in equation (2.7) and (2.5) are the same because the dark current due to diffusion is also the leaky current in an ideal diode.

Other contributions to the dark current are material defects in the depletion region caused by Shockley-Read-Hall generation processes.

2.1.5 Responsivity

Photodiodes are characterized by their responsivity. The responsivity of a photodiode can be estimated from fundamental constants, the wavelength of radiation, the reflectance and internal losses of the photodiode. A simple definition of responsivity is that it is the ratio of radiant power incident on the photodiode to the photocurrent output. The silicon detector used in this project is modelled as an ideal quantum detector with, as mentioned before, two loss mechanisms: the reflectance and IQD.[16] This gives the following equation for R:

$$R(\lambda) = \frac{e\lambda}{hc} (1 - p(\lambda)) * (1 - \delta(\lambda)) \quad (2.8)$$

where e = elemental charge, h = Planck's constant, c = speed of light in vacuum and $p(\lambda)$ = spectral dependent external losses and δ = IQD.

2.1.6 Internal quantum deficiency

The formal definition of Internal quantum deficiency (IQD) is: "the relative number of absorbed photons not producing charge carriers collected by the external measurement circuit".[3] Basically meaning the photoelectrons not registered by an external form of voltmeter. The losses in a photodiode comes from external losses (like reflected losses, absorption by the passivation layer, absorption by unwanted dust on top of the diode) and IQD, with the last one referred to as a recombination of photogenerated electron-hole pair.[1] IQD is calculated with the relation:

$$IQD = 1 - \frac{R_{surf} + R_{bulk}}{G_{opt}} \quad (2.9)$$

where R_{surf} = total surface recombination, R_{bulk} = total bulk recombination and G_{opt} = total photogeneration.

An approximation for IQD can be found through current by the expression:

$$IQD = \frac{1 - I(V)}{I_{ph} - I_{dark}} \quad (2.10)$$

In equation (2.10) the terms under the denominator are the max-values.

One important part regarding improvement of photodiodes is decreasing IQD as much as possible. Equally important is the fact that it gives the possibility to predict the loss and compensate for it. Bulk and surface recombination is further elaborated on in section 4.1.

2.1.7 Uncertainty of Photodiodes

The uncertainty of a measurement expresses the doubt about how well the measurements represents the value of the measurement.[17] It is a major issue in all fields of measurement. Despite being a rather general concept that takes into account a wide variety of issues like random and systemic errors, it has a quantitative approach where the standard deviation of a measurement represents its value. The standard deviation is given in ppm. Previously, it has been pointed out that the intention is to decrease the uncertainty to below 10 ppm in order to get a new standard for measuring the optical constant based on constant parameters in equation (2.7) for example.

The uncertainty is divided in two: type A and type B. Type A is the observed variation in the measurand often expressed as the standard deviation and given by the relation:

$$s = \sqrt{\frac{1}{n-1} \sum (x_i - \bar{x})^2} \quad (2.11)$$

where n = number of measurements, x_i = the measurement in question and \bar{x} = mean or expectation value.

Type B is based on all the relevant information available, like manufacturer specifications and data provided in calibration reports. In the project, the emphasis will be put on type A uncertainty.

By decreasing the ppm to 10 or below, preferably 1 ppm, the uncertainty could be lowered so much that the ratio between the incident photons from an optical laser and the value read at an detector would be 1:1.

2.2 Comparative simulations from JV

Simulations are important tools for evaluating and designing new photodiodes. The simulations have the potential to provide new insights in their functionality and give opportunity

to design the diodes for use in extreme environment, like under CT. And at the JV many important simulations have been done and in this section those simulations will be described in more detail in order to compare them with the experiments done in this project.

Perhaps the basis of all the simulations done by JV came in 2011 with the simulation of the PQED. The program used was PC1D, a primitive version compared to the newer simulation-platforms. And the values and parameters required for running the simulation were either received from the factory (like wafer thickness) or assumed (like optical power). The effective lifetime is given according to equation (2.21).[18]

At 77 K; the simulation showed a low IQD for the PQED, especially at short wave-

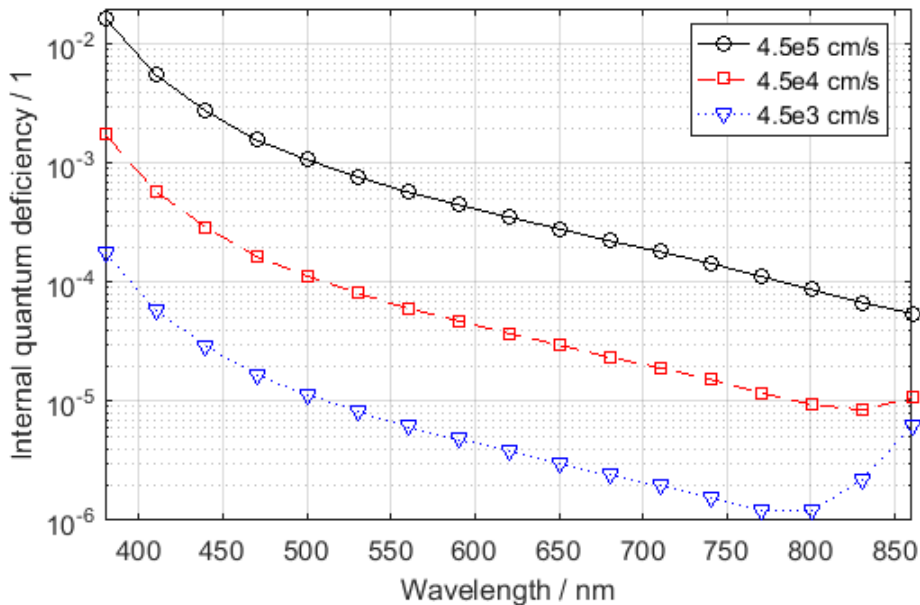


Figure 2.5: Simulated Internal quantum deficiency as a function wavelength for different SRV parameters. Image provided at the courtesy of Chi Kwong Tang.

lengths. While at long wavelengths, the IQD increased. This circumstance became more evident as the temperature increased. However, when compared to other similar software tools, it showed an uncertainty for IQD 10 times lower than it should. So any value for IQD should be multiplied with that amount. Despite that, the results were positive and relatable for this project. In 2015 Tang et al. measured and 3D modelled the IQD of an oxide-charged induced junction photodiode at RT. The 3D simulation model was investigated under different conditions and compared with recent experiments. Result-wise, it showed good agreement and could therefore be used as an adequate simulation model. JV found that the IQD is mainly limited by the surface quality at low optical power. With a good surface, a IQD at 10 ppm could be obtained by the simulations.

Wavelength (nm)	IQD (ppm)	Voltage (reverse bias)	Temp (RT/CT)
800	< 100	- 5V	RT
600	< 1	- 5V	CT

Table 2.1: Table over simulated IQD. It should be pointed out that all the results are predictions

Cogenda Genius was the software used and the photodiodes were made of a p-type high resistivity silicon with a thermally grown oxide layer. The optical power, was in the simulations, a stabilized laser source of respectively 407, 532 and 850 nm. With regards to the IQD, this was calculated from the extracted ratio between the total optically generated and the total recombined ehp.[19]

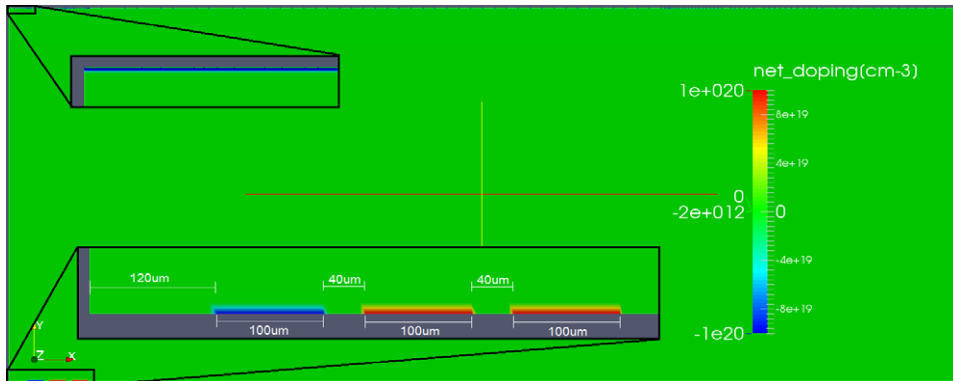


Figure 2.6: Schematic of how the induced junction diode on figure 2.2 is designed in Cogenda Genius. Schematic provided at the courtesy of Chi Kwong Tang

Another Cogenda Genius-simulation was performed in 2017 when Tang et al. attempted to extract the SRV parameters of SiN_x -passivated p-type silicon. SRV for electrons (SRVn) and holes (SRVp) are difficult to obtain directly from experiments, so reliable device simulations can facilitate the access of the parameters. The reason for the importance of the parameters is that they are necessary to predict the responsivity of a photodiode when exposed to an optical power. A self-consistent solution between the Poisson equation ($\nabla^2 p = f$), eh continuity equations and sum of all recombination is iterated by the simulation software. The parameters were: fixed charge density, SRVn, SRVp and SRH bulk lifetime.[20] Simulations showed that the fixed charge density and SRVp can shift curves in opposite directions by the injection level. It also showed that at injection levels below $2 \times 10^{15} \text{ cm}^{-3}$, the simulation results are in complete agreement with the experiment, but otherwise are not.

A major improvement in simulating the PQED came with Jarle Gran et al. and the JV teams 3D device simulation and measurement of a p-type PQED. The simulation results

showed that the IQD could be decreased to below 1 ppm if the SRV for electrons and holes is brought down to a sufficiently low value. Measurements were done in both RT and CT and the default simulations parameters were (given in table 2.2):

The simulation confirmed that SRV dominated at short wavelengths, while bulk recombination dominated at long wavelengths. For the optical excitation a power stabilized at 488 and 633 nm was used. The values for SRV are in the range of the passivation layers that were briefly explained earlier. With a SRV below $4e3$ cm/s and 800 nm illumination, a IQD below ppm was achieved with simulation.

More relevant for this project, a simulation with the default parameters, but with a slight adjustment in the temperature to 77 K, gave a decrease in SRV by a factor of 10.[1] It also showed that the bulk recombination could experience a similar reduction by increasing the reverse bias voltage to - 10V. Worth mentioning is also the result that the IQD increases at low voltage with decreased illumination area. It means that the linear region (where IQD saturation voltage can be found) can be extended by increasing the illumination area or by decreasing the temperature to CT.

The last point to include is the results found with regards to fixed charge density; for the performance of a photodiode it is very beneficial to increase the fixed charge. An improvement by a factor of 2 in IQD can be obtained and a significant improvement in linearity when cooled down to CT. This can be seen in figure 2.7 where a simulation is conducted for IQD as a function of the wavelength. It clearly indicates a much lower IQD in ppm for the PQED at CT compared to the PQED at RT.

Table 2.2: The default simulation parameters in the simulation, e symbolizes the potency 10.[1]

Parameter	Value
Temperature	300 K
Substrate doping, N_D	$2e12 \text{ cm}^{-12}$
Fixed charge density, Q_f	$6.2e11 \text{ cm}^{-2}$
Reverse bias voltage	- 5V
SRH bulk lifetime, τ	4 ms
Surface recombination velocity, S_0	$1e5 \frac{\text{cm}}{\text{s}}$
Illumination area	$1.5 * 1.5 \text{ mm}^2$
Absorbed optical power	$500 \mu \text{W}$

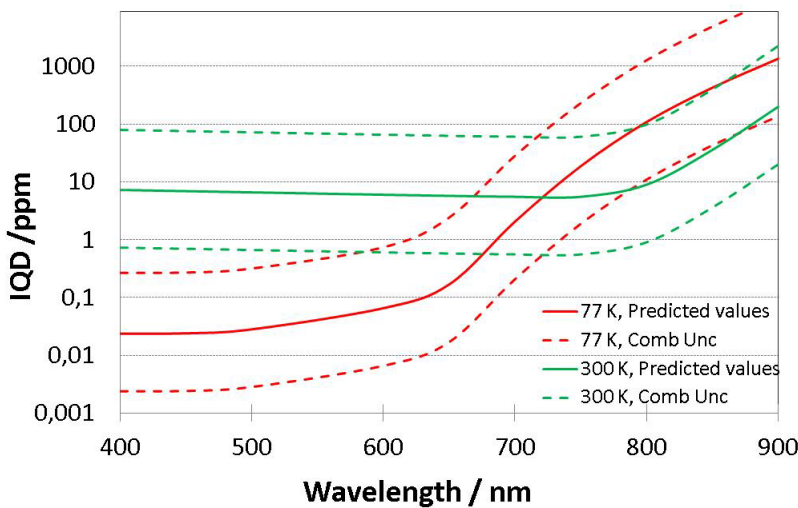


Figure 2.7: Schematic of IQD as a function of wavelength for both CT and RT conditions. Red color indicates CT and green RT. Figure provided at the courtesy of Chi Kwong Tang

2.3 Cooling of diodes

Cooling of photodiodes is done rather frequently in industrial and scientific processes in order to reach target goals like reducing dark current and IQD.[2] These tasks are accomplished with a variety of techniques, but in this project the focus will be on cooling by liquefied Nitrogen (N_2). For a commercial photodiode the IQD seems to be limited to 1 - 0.1 %.[21] Geist et al. suggested in 2003 that smaller uncertainties could be obtained with induced photodiode reflectance traps constructed from custom photodiodes under reverse bias at cryogenic temperatures.

Based on this the JV and collaborators created the PQED that supposedly gives a significant improvement in uncertainty.[22] The numbers suggested were 80 ppm in RT and spectacularly only 10 ppm at CT, with the possibility of further decrease based on simulations.[1] An another improvement was that no voluminous cryogenic radiometer was necessary.[22] A similar research on minority carriers in n-type Si by Pere Roca et al. showed a drop in lifetime values.[23] Specifically a decrease in radiative and Auger lifetimes, while an increase in SRH lifetime was observed. Surface recombination is due to defects and increases, and also worth noticing: effective lifetime at 77 K is dominated by bulk recombination. The last aspect seen was an alteration of light excitation and intrinsic properties under the change of temperatures.

Chapter 3

Photodiode experiments and results

3.1 I-V measurements at Justervesenet

The I-V measurements show the relationship between current and voltage in an electronic device. Figure 2.4 shows this for a photodiode. The trajectory for a photodiode is non-linear (more exponentially actually), as can be witnessed in the figure, in stark contrast to electronic components like a resistor which is linear in the relationship between current and voltage.

In this project, measurements of photodiodes at RT and CT are done to acquire data of the performance of real photodiodes at different temperatures with regards to linearity and internal losses. The data are acquired using an in-house developed LabView program to control voltage source and multimeters. Datron 4700 was used as the voltage source and Keithley 2000 was the multimeter. The induced junction diode is the test sample. All the experiments have been made with a transimpedance amplifier with a gain setting of 10^3 V/A. Important in this regard is to limit the noise from the circuit in general, as well as the noise from specific components like amplifiers.

With the equipment there are several factors that need more proper explanation. The instrument has 3 main modes for frequency based on the number of power line cycles (NPC): slow (10 NPC), medium (1 NPC) and fast (0.1 NPC). Based on preliminary test and the standard deviation, slow mode gives the best signal to noise ratio.

Other parameters that are possible to manipulate are the integration time and the following delay which also is an input value. The setup has two lasers; one red (633 nm) and one blue (488 nm). Every complete measurement consists of light reading and dark reading that alternate. If there is an integration time of 25 s and delay time of 10 s, one reading has the duration of 35 s. With a reverse bias voltage of - 10V and step 0.2, 50 measurements are anticipated. Multiplying that with the time per measurement, combined spent time will be equivalent to $70 \text{ s/measurement} * 50 \text{ measurement} = 3500 \text{ s}$.

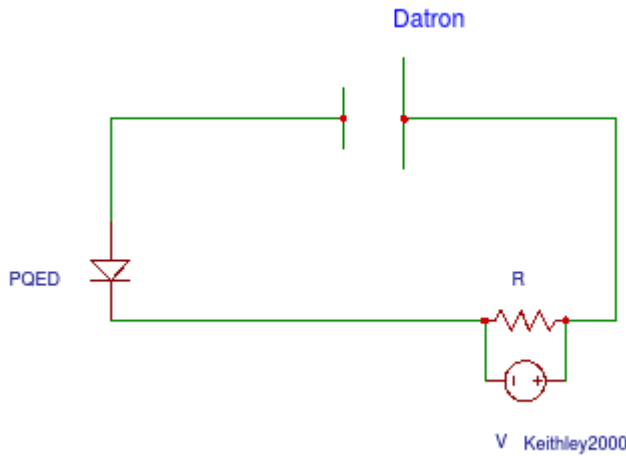


Figure 3.1: Schematic of the circuit used in the JV laboratory

Perhaps the final way to vary the I-V system is through filters. The instrument has two methods: moving average and repeating filter. Filter can be used to stabilize the measurements even further. Moving average is the main filter used and it is based on an average of the measurement, as exemplified in the following with filter of 10: when 10 measurements are read, an average of 1-10 is done. When an another measurement is added, an average of 2-11 measurements is done. For the repeating filter, the system gets cleared after the 10 measurements. The next array is therefore 11-20 measurements.

3.1.1 Laser setup at JV

The photodiode was placed in the JVs laser setup. The diode is inside a LN2 cryostat that gets exposed to polarized laser. As seen on figure 3.2 (I), the photodiode is attached to the cryostat and can be measured at any temperature between 300 and 77 K. This metal rod is also attached to the photodiode. So basically when the rod gets cooled down by the LN2, then the diode also gets colder. Based on this a temperature close to 77 K was reached.

3.2 I-V experiment

In this section the experiment is explained.

1. A laser setup is set up as imaged in figure 3.2.
2. All necessary input parameters are added. These are slow frequency mode and amplification by 10^3 m moving average filter.

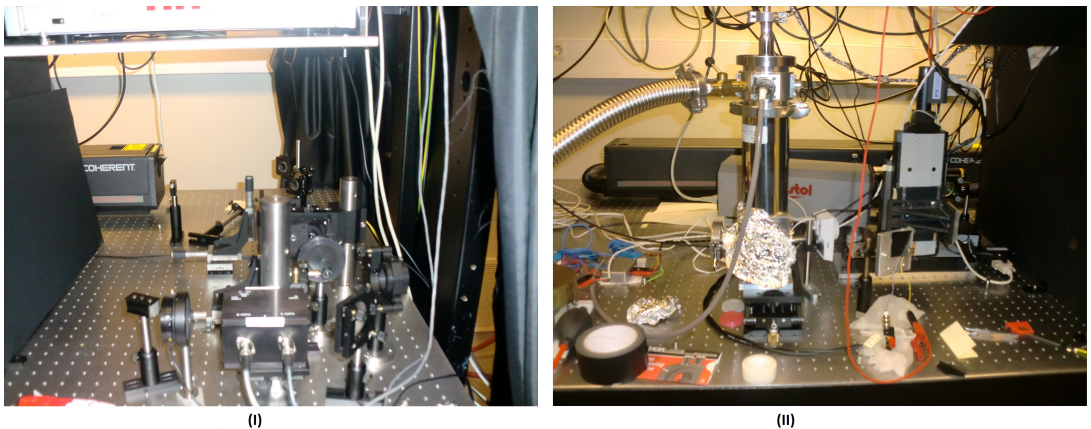


Figure 3.2: Picture montage of the laser setup at JV. (I) Optics to clean and align the laser. A shutter and a power stabilizer is visible near the bottom of the picture. (II) Cryostat with the detector inside.

3. All the parameters from table 3.1 are added. The parameters are integration time, delay, initial, voltage and step.
4. LN2 is added to the dewar until it is filled up. If the measurement has a long integration time, more refills are needed during the experiment. If the experiment is done in RT conditions, then obviously step 4 is superfluous.
5. Light in the room is turned off and measurement commences by starting it in the software.

3.3 Results

With the laser setup at JV, the target was to compare CT and RT performance of the photodiodes. The measurements were done on an induced photodiode with a SiO_2 passivation layer. In the figure 3.3, the I-V characteristic both CT and RT are presented with blue = CT and red = RT. The experimental parameters are as following:

Input parameter	Values
Integration time (s)	25
Delay (s)	10
Initial voltage (V)	-10
Step	0.2
Wavelength (nm)	633
Power level (mW)	1.5

Table 3.1: Table shows the input parameters for the experiment conducted at JV

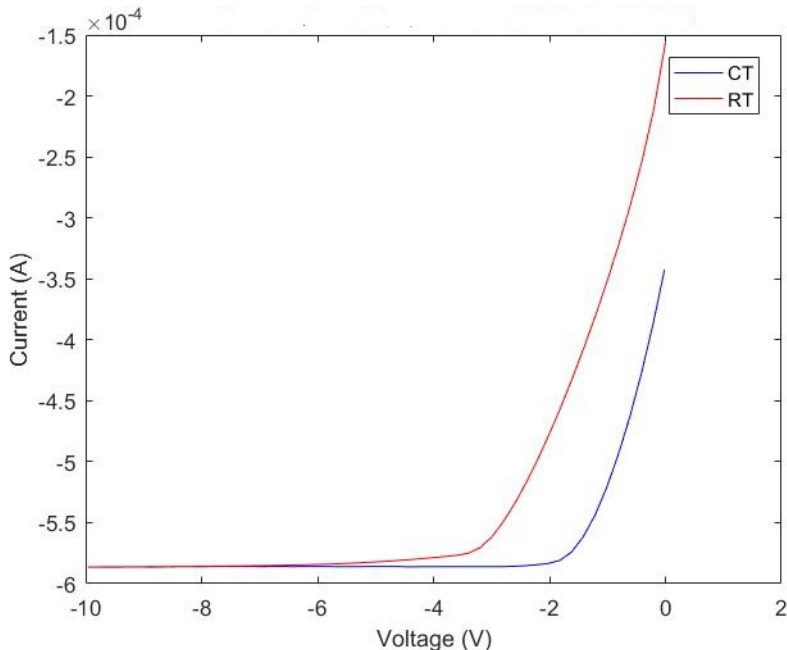


Figure 3.3: I-V curve with the parameters and $1500 \mu\text{W}$ in optical power as given and with blue line = CT and red line = RT, since they traditionally symbolizes those colours.

In figure 3.3, the curves for the two temperatures are slightly different from each other. While the one for RT follows the traditional exponential like slope for photodiodes as seen on figure 2.4, the one for CT follows a linear flat path for a longer period in the given interval from -10V to 0V. A better linearity for lower voltages is therefore seen for CT conditions compared to RT conditions. Compared to previous simulations from JV the results confirm the results obtained from the simulations.

With regards to the internal losses of photodiode, it could be found on the signal with

the equation (2.7). The following relation for uncertainty U;

$$U = \sqrt{s_{current}^2 + s_{dark\ current}^2} \quad (3.1)$$

where s = standard deviation gives a type A uncertainty. There were 2 different samples with the same parameters. One of them were done under CT conditions, while the other one had RT conditions. The plot is so done with the voltage on the x-axis and the uncertainty on the y-axis. It is clearly indicated from the plot on figure 3.4 that the uncertainty

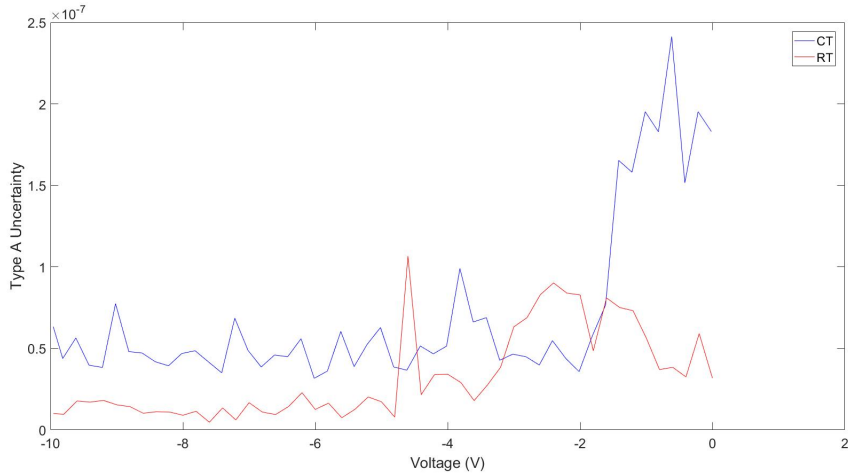


Figure 3.4: Schematic of the type A uncertainty as a function of voltage for both cryogenic and room temperature. Red = RT and blue = CT

for RT becomes higher compared to CT from the - 5V and on. Before that the difference is negligible. The highest voltage values could be considered neglected due to the high noise values at such voltages. But from -5 V and above, there is a clear difference. This suggests that a photodiode under CT would have values close to those expected from the simulation. And they are lower than those for RT. However, it should also be pointed out that the uncertainty does not decrease as clearly as expected with CT measurements as suggested from the simulations. More testing with diodes with other passivation layers is needed to make a complete confirmation of this fact though.

The values on the y-axis clearly gives that the uncertainty is at the 10^{-7} scale which is below our desired values at 10 ppm and shows great promise for achieving a 1:1 ratio between incident photons and detected photons.

While the uncertainty is the actual size of the uncertainty in the units used to measure it, a term from statistics, relative uncertainty, calculates the ratio of uncertainty to the value measured. Relative uncertainty in this regard is given by:

$$U_{rel} = \frac{\sqrt{s_{current}^2 + s_{dark\ current}^2}}{I_{current} - I_{dark\ current}} \quad (3.2)$$

The plot for equation (3.2) is given in figure 3.5 for both CT and RT conditions.

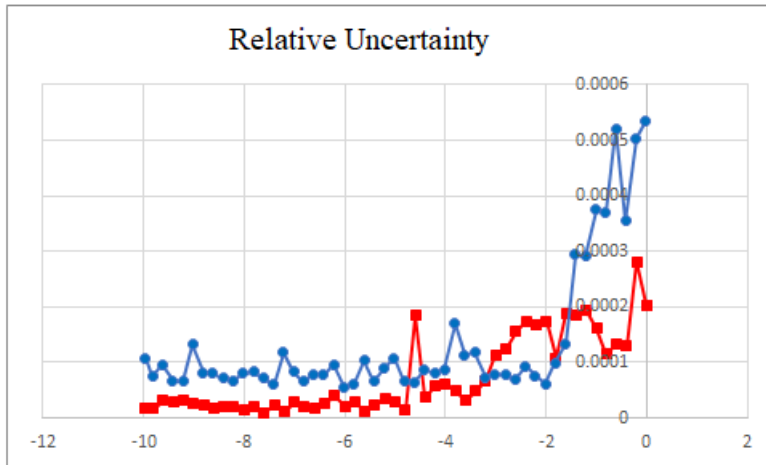


Figure 3.5: Schematic of the relative uncertainty for CT=blue and RT=red. X and y-axis lack axis-labels due to overprocessing in the Excel-file. X-axis = voltage and y-axis = IQD.

The schematic of the relative uncertainty in figure 3.5 confirms the values obtained from the uncertainty measurements from figure 3.4. PQED at CT has a slightly higher IQD throughout the plot, but these values could be artefacts or noise. The difference is negligible and the IQD is still below the desired value of 1 ppm. It also reinforces the thought that an improved linearity is the only gain from decreasing the temperature to CT.

3.4 Summary of the I-V measurement results

The section will provide a summary of the I-V measurement results.

- An improved linearity for lower voltage was expected based on simulations. The results confirmed this.
- No change in current when measurements are done at CT conditions compared to RT conditions. Theory indicated that a better signal was expected. However, this did not occur.
- IQD does not decrease at CT. On figure 3.4 with identical parameters, the two measurements only deviate from each other at -5 V and up to 0 V.
- Relative uncertainty confirms the results from the uncertainty plot.
- Achievable uncertainty for the induced junction diode is at 1 ppm.

3.5 Relationship between I-V experiments and recombination experiments

As a prelude to the next sections, an explanation will be given for why the I-V experiments at JV and recombination experiments at Institute for Energy Technology (IFE) are so interconnected and why recombination experiments can help to improve the performance of the photodiodes.

In the simulations, it was indicated that decreasing the recombination was the main contributor to decreasing the IQD to below 1 ppm at CT. The results, seen in the I-V curves in this chapter, proved that IQD had in fact decreased significantly. To be able to verify that the recombination is the factor increasing the performance at CT, experiments on Si-wafers with passivation layers used in the diode has to evaluated. In that regard, passivation layers that might improve the lifetime even more than the ones used in the PQED, might also be analyzed for comparison. The photodiode experiment suggests that the SRV at CT and RT are not the same. Since they are not the same, interest around the study of SRV at CT (or the recombination experiment in other words) increases dramatically.

Recombination and characterization theory

4.1 Lifetime of carriers

In 1952 a theory of electron-hole pair recombination through recombination centers was put forward.[4] Recombination is defined as the time it takes for an electron-hole pair (ehp) to cease to exist on an average time τ , while generation occurs when a semiconductor is exposed to light with photon energy larger than the band gap and excited charge carriers are created in the material.[7] This two-way phenomena is interconnected and a free-electron in the conduction band of semiconductor has to combine with a hole for the system to return to equilibrium after the optical generation. The phenomena can be seen in both the bulk and on the surface. In the early days of the semiconductor industry a limitation of the bulk recombination was sought after, but as the size of the transistors used in modern electronics decreased down to below millimeter scale, the surface passivation become more important.[24][25] But despite that a thorough explanation of both the bulk and surface recombination is necessary since the experimental effective recombination is based on both of them. As already explained in the introduction, ehp recombination is the main force limiting the responsivity of a photodiode.

4.1.1 Bulk recombination

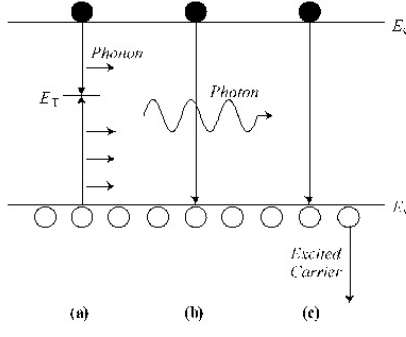


Figure 4.1: Recombination mechanisms:(a) SRH, (b) radiative, and (c) Auger.[4]

Bulk recombination is given by three main mechanisms: Band-to-band radiative recombination, Auger recombination and Recombination via defects (SRH-recombination). The recombination is given by:

$$R = \frac{\Delta n}{\tau} \quad (4.1)$$

where Δn = excess carrier density in p-type. Equation (2.8) and the information in the paragraph above leads to:

$$R_{bulk} = R_{rad} + R_{Aug} + R_{SRH} = \frac{\Delta n}{\tau_{rad}} + \frac{\Delta n}{\tau_{Aug}} + \frac{\Delta n}{\tau_{SRH}} \quad (4.2)$$

The lifetime then becomes:

$$\frac{1}{\tau_{bulk}} = \frac{1}{\tau_{rad}} + \frac{1}{\tau_{Aug}} + \frac{1}{\tau_{SRH}} \quad (4.3)$$

In the following section, a closer inspection of the three mechanism is done.

Radiative recombination Before continuing with the text, a referral to figure 4.1 is mandatory in order to further the understanding for the reader. In radiative recombination ehps gets annihilated (they recombine from band to band) with the energy removed by a photon.[4] The radiative lifetime is given by:

$$\tau_{rad} = \frac{1}{B_{rad} N_A} \quad (4.4)$$

since we experience low injection conditions with the induced diode. B_{rad} is a material specific coefficient and N_A is the amount of acceptor doping. The radiative recombination rate for Si is very small due to the fact that Si has an indirect bandgap.

Auger recombination In an Auger recombination, a electron and hole recombine and transfer their excess energy to either an electron in the conduction band or a hole in the valence band.[7][24] That suggests that a prerequisite for defining the Auger recombination is the involvement of a third charge carrier that receives the excess energy. The expression for Auger lifetime is, with the parameters; low injection and p-type material.

$$\tau_{Aug} = \frac{1}{C_p N_A^2} \quad (4.5)$$

where C_p is the Auger coefficient for holes. Auger recombination is very dominant in Si-wafers that are heavily doped, but not necessarily so for the lightly doped. This is due to the coulombic interaction of the charge carriers that causes an enhancement of the recombination rate.[7]

Recombination via defects is also called the SRH recombination after its founders; Shockley, Read and Hall. From material science it is known that defects exist in crystalline materials. The defects are classified after their dimension with a domain from zero to three. These defects are for example point defects like vacancies, substitutional and interstitial impurities, line defects like dislocations (or lack of a plane of atoms) and surface defects like grain boundaries. The defects could be of both intrinsic or extrinsic nature.

They are important because they have the ability to function as recombination centers, and they can produce discrete energy levels within the band gap. Discrete energy levels go so on to increase the recombination rate because of the electrons tendency to relax from the conduction band to the defect level and then conduct further relaxation to the valence band where it proceeds to annihilate the a hole.[7] If a defect level is close to the band edge level in energy, the probability for the process is further increased for respectively electrons close to the conduction band and electrons close to the valence band. These energy levels are called dopants when the defects are very shallow, traps for shallow defects and deep defects are referred to as recombination centers. It should also be mentioned that lines between them is blurry.

The SRH lifetime of a single defect is given by the relation:

$$\tau_{SRH} = \frac{\tau_{n0}(p_0 + p_1 + \Delta n) + \tau_{p0}(n_0 + n_1 + \Delta n)}{p_0 + n_0 + \Delta n} \quad (4.6)$$

Equation 4.7 is dependent on injection level, doping concentration, defect parameters and temperature. τ_{n0} and τ_{p0} are the capture time constants of electrons and holes. In (4.7) n_1 and p_1 are defined as the SRH equilibrium densities of electrons and holes when the Fermi level, E_F , coincides with the defect energy E_t .[26] They are expressed by:

$$n_1 = N_C * \exp\left(-\frac{E_C - E_t}{kT}\right), p_1 = N_V * \exp\left(-\frac{E_t - E_V}{kT}\right). \quad (4.7)$$

The expression becomes:

$$\tau_{SRH} \approx \tau_{n0} = \frac{1}{\sigma_n N_t v_{th}} \quad (4.8)$$

where σ_p = capture cross section for holes, N_t = defect concentration and v_{th} = carrier thermal velocity.

The traps are further divided into shallow and deep-level defects. Difference between the deep and shallow-level defects is the amount of energy needed to remove an electron or hole from the trap to the valence or conduction band.

4.1.2 Surface recombination

A crystalline material like c-Si is built up according to a periodic pattern with a unit cell that repeats itself throughout the bulk of the material. At the surface this tendency is interrupted since surface atoms lack neighbours to bind to, and as such are left as unsatisfied "dangling" bonds.[5] This term reflects on the fact that the Si-atoms are only partially

bonded. The unsatisfied Si atoms introduce energy levels called surface states inside the forbidden semiconductor band gap. Recombination increases significantly due to this factor.

Earlier in the text it has been pointed out that the bulk recombination defect states have discrete energy levels. For the surface recombination this is not the case. This leads to the expression for surface recombination:

$$R_s = (n_s p_s - n_i^2) v_{th} \int_{E_V}^{E_C} \frac{D_{it}(E)}{\frac{n_s + n_1(E)}{\sigma_p(E)} + \frac{p_s + p_1(E)}{\sigma_n(E)}} \quad (4.9)$$

where n_s and p_s = electron and hole concentration respectively at the surface, D_{it} = areal density of the surface states. E_C = energy for the conduction band and E_V = energy for the valence band.

Instead of lifetime, a term called surface recombination velocity (SRV) is used. SRV is defined as the surface recombination divided by excess carrier.[7] Thereby the equation of SRV is:

$$\frac{1}{S} = \frac{\Delta n_s}{R_s} \quad (4.10)$$

It should also be pointed out that n_1 and p_1 could be neglected in inversion or if one excess carrier is dominating. One could simplify the recombination rate to:

$$R_s = \frac{S_{n0} S_{p0} (n_s p_s - n_i^2)}{S_{n0} (n_s + n_1) + S_{p0} (p_s + p_1)} \quad (4.11)$$

where $S_{n0} = \sigma_n N_{it} v_{th}$ and $S_{p0} = \sigma_p N_{it} v_{th}$.

In order to further the understanding of the subject, two scenarios are studied, with their names given in parentheses: one with no electric field near the surface (flat band condition) and one where there is an electric field near the surface (band bending due to surface charges). For flat band conditions, the band structure is similar to the bulk, meaning $n_s = n$ and $p_s = p$. In a p-type sample with low injection, the SRV becomes:

$$S = v_{th} \int_{E_V}^{E_C} D_{it}(E) \sigma_n(E) dE \quad (4.12)$$

At low injection the total recombination rate is limited by the capture of minority carriers only, since the majority carriers are in great excess.[7]

For the second scenario, surface bending: there exists an electrical field in proximity to the surface due to charged ions or fixed charges in the dielectric layers. This region could for example be an accumulation layer or an inversion layer depending on whether it is a majority or minority carrier (for our instance minority of course).

As already shown in figure 4.2 there are fewer electrons and holes in the surface compared to the bulk, so this electrical field gives a skewed number of electrons and holes. In

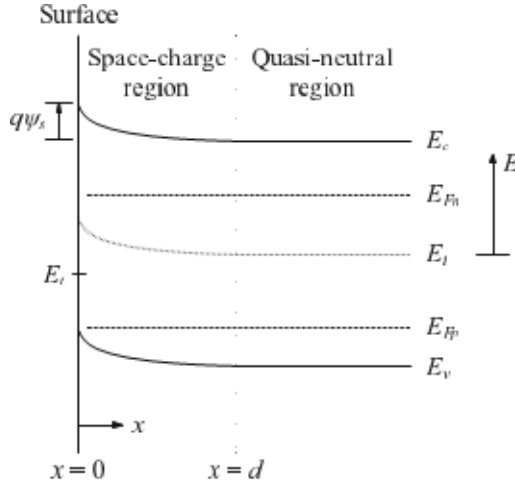


Figure 4.2: Band diagram of the (p-type) silicon surface under non-equilibrium conditions, and with non-zero surface band-bending (accumulation), showing definitions of relevant energies and potentials.[5]

figure 4.2 a bending of the semiconductor energy band is seen. The bending is given by ψ_s . For a downward bending like in the figure, ψ_s is positive. As the distance from the surface gets larger, a charge neutrality is seen and a quasi-neutral region is created. It is possible to calculate the surface carrier concentration based on the extent of the bending of the band. For the interested reader, a derivation of the equation can be found in literature found elsewhere, but for the project it suffices to give:

$$p_s = Q_s^2 \frac{1}{2kT\epsilon_s} \quad (4.13)$$

where Q_s = total charge of space-charge region, kT = Boltzmanns constant multiplied with the temperature and ϵ_s = vacuum permitivity at the surface.

Experimentally, the parameter measured is not SRV, but the excess minority carrier lifetime. τ_{eff} is a superposition of all the recombination methods described up to this point. The expression becomes:

$$\frac{1}{\tau_{eff}} = \frac{1}{\tau_{rad}} + \frac{1}{\tau_{Aug}} + \frac{1}{\tau_{SRH}} + \frac{1}{\tau_s} \quad (4.14)$$

where the new addition τ_s is, in a symmetrically passivated undiffused wafer:

$$\tau_s = \frac{W}{2} \frac{\Delta n}{R_s} \quad (4.15)$$

where W = wafer thickness and R_s = recombination at each surface.

4.2 Passivation and materials

As the intention is to limit recombination as much as possible, it is worth making a summary of the last section: theory indicates little τ_{rad} because Si has an indirect bandgap, τ_{Aug} will also have limited input since a low-doped injection diode is used. And τ_{SRH} is dependent on defects functioning as recombination centers with a certain energy. The relevant materials used in this experiment are: Si, oxide, and nitride.

4.2.1 Surface passivation - background

Surface passivation is considered to be the act of reducing recombination of a surface.[5] For clarity's sake it should be pointed out that one wishes to increase the effective lifetime of the wafer. This can be done by either reducing the number of surface states or by reducing the concentration of minority carriers. With regards to the latter method of reducing the minority carrier concentration, this is done by using the induced junction diode. An another method is to use the field-effect passivation which is done by using charges to change the surface potential and thereby the surface concentration of electrons and holes.[7]

According to equation (4.7), the surface recombination is proportional to the density of states at the surface, D_{it} . By depositing a surface passivation layer on top of the semiconductor material, this parameter can be significantly reduced. Process-wise, a thin layer is deposited so that the previously mentioned "dangling" bonds chemically bind to atoms in the layer and become satisfied. Dielectric materials like SiO_2 , SiN_x and Al_2O_3 are used for the thin passivation layer. Some research has led to a reduction in states from 7×10^{14} surface atoms/cm² to 10^9 surface atoms/cm² for a bare (100)-oriented Si-surface.[7] It should be mentioned that the "fixed charge" from figure 2.3 also contribute to the charge-assisted surface passivation. The next subsection will give further explanations relating to the materials used as passivation layer. One of the main aspects of this assignment is to find out what material gives the highest lowering of the recombination at cryogenic temperatures.

4.2.2 SiO_2 passivation

When calling upon an oxide layer as a passivation layer, we in fact create a Si-SiO₂ interface by the deposition of a thin SiO₂ film on top of a Si-wafer. An oxide layer was actually the way Attala et al. discovered that a dielectric layer greatly reduced the amount of electronic states at the Si surface.[5] For many decades it was also the industry standard concerning dielectric films.

It has previously been shown that SiO₂ significantly decreased the number of density states. The defect states could be further reduced through an annealing in H₂ ambient.

4.2.3 SiN_x passivation

An alternative to oxide as a passivation layer is SiN_x. It is deposited almost exclusively by PECVD and consists of silicon and nitrogen. As the name indicates x denotes the

nitrogen/silico atomic ratio and its precursor often involves hydrogen, like SiH_4 and NH_3 . It can be deposited at low temperatures and in big quantity. SiN_x not only functions as a surface passivation layer, but can induce bulk passivation of the Si-wafer as well. The effect can be obtained by a thermal activation of the layer where hydrogen diffuses from SiN_x to the wafer and passivates defects. A study by Soppe et al. indicates that the effective lifetime increases at the highest temperatures due to the combined bulk and surface passivation.[27] Basically the opposite of the intention in this project. Because of this nitrid is commonly used as a dielectric layer for solar cells, mainly based on the following properties: a large positive fixed charge density that suits optimally for n-type emitters, optical properties as an antireflection coating with refractive index at $n = 1.8$ and above and finally the large hydrogen concentration that increases the effective lifetime.

4.3 QssPC for lifetime measurements



Figure 4.3: An image of the WCT-120 instrument used for QssPC measurements.[6]

interface) is not required. They are also opportune for this project due to the researchers approach based in the interest in appreciating increased lifetime.[6]

So the above heavily implies that the work will be done with the transient method. The method has four parts. One starts out by subjecting the sample to a short pulse of light

The QssPC measurements were done on a WCT-120 from Sinton Instruments. The instrument uses an eddy-current conductance sensor and a filtered xenon flash lamp to measure carrier lifetime. The entire system also includes optical filters and a computer with excel: the results are given by Microsoft Excel since it has a function with macros built in. From a purely practical point of view the process is along these lines: one places the wafer on top of the clearly indicated sensor, do a calibration and measure the effective lifetime as a function of injection level.

The instrument has 4 basic modes: QssPC, general 1/1, general 1/64 and transient. If the assumed lifetime range exceeds roughly $200 \mu\text{s}$ and above, the preferred modes of measurement are transient and generalized 1/64. In these modes the optical constant (can be estimated from known values of absorption coefficients and refractive indices of the Si-passivation layer

that peaks and decays back to darkness rapidly.[6] Typically it last 100-200 μs . After the flash has finished, the second part is due. The decay of the sheet conductance is measured as a function of time. This sheet conductance goes further on to be converted into an average excess carrier density Δn . Last part in the method is to take the derivative of the conductivity with respect to time.

$$\tau = -\frac{\Delta n(t)}{\frac{d\Delta n(t)}{dt}} \quad (4.16)$$

where Δn = excess carrier concentration and $\frac{d\Delta n(t)}{dt}$ = derivative of conductivity.

With the QssPC the intention is to show that the SRV decreases with the temperature. Then we see that there is potential to reach our goal for the wafer. Photodiode-structure takes a while to create due to the complexity of the process with PECVD deposition of passivation layer, contacting and etching from wafer to photodiode. The diodes are limited by the surface recombination.

A requirement for the QssPC to properly work is that the lifetime has to be far above the flash turn off time, which means basically above 100 μs for valid results. The result is also largely independent of the light intensity and optics. Calibration of the instrument to adjust to the measurement stage developed is also mandatory since the values would be greatly skewed and irrelevant if otherwise.

4.4 QssPC measurement stage

Due to the fragility and high cost of the equipment used to measure Si-wafers, a measurement stage had to be developed and constructed. The reasoning for this is that decreasing the temperature to 77 K with liquid N₂ could possibly damage expensive equipment. A measurement stage had to be developed for each of the measuring techniques. Lots of ingenuity and conversations with people familiar with similar experiments was required.

From a technical standpoint, the measurement stage had to be built with specifics that had to take into account that the measuring equipment had to be protected, as well as fulfilling the parameters for obtaining a good and valid measurement into its design. Those parameters were for example what material could withstand the low temperature without breaking apart (basically meaning that it had to have a low thermal expansion coefficient), if a N₂ reservoir was required and if the sensor on the QssPC had its detection power altered.

Before going further into the details, the figure 4.4 should be referred to. The entire process of measuring QssPC under cryogenic conditions goes according to the picture slide in the figure. The picture montage also shows how the measurement stage is built up.

First of all a calibration is done with 5 wipes and a petri dish on top of the sensor. The standard for the instrument is to use 4 reference wafer with 4 different resistivity

4.4 QssPC measurement stage

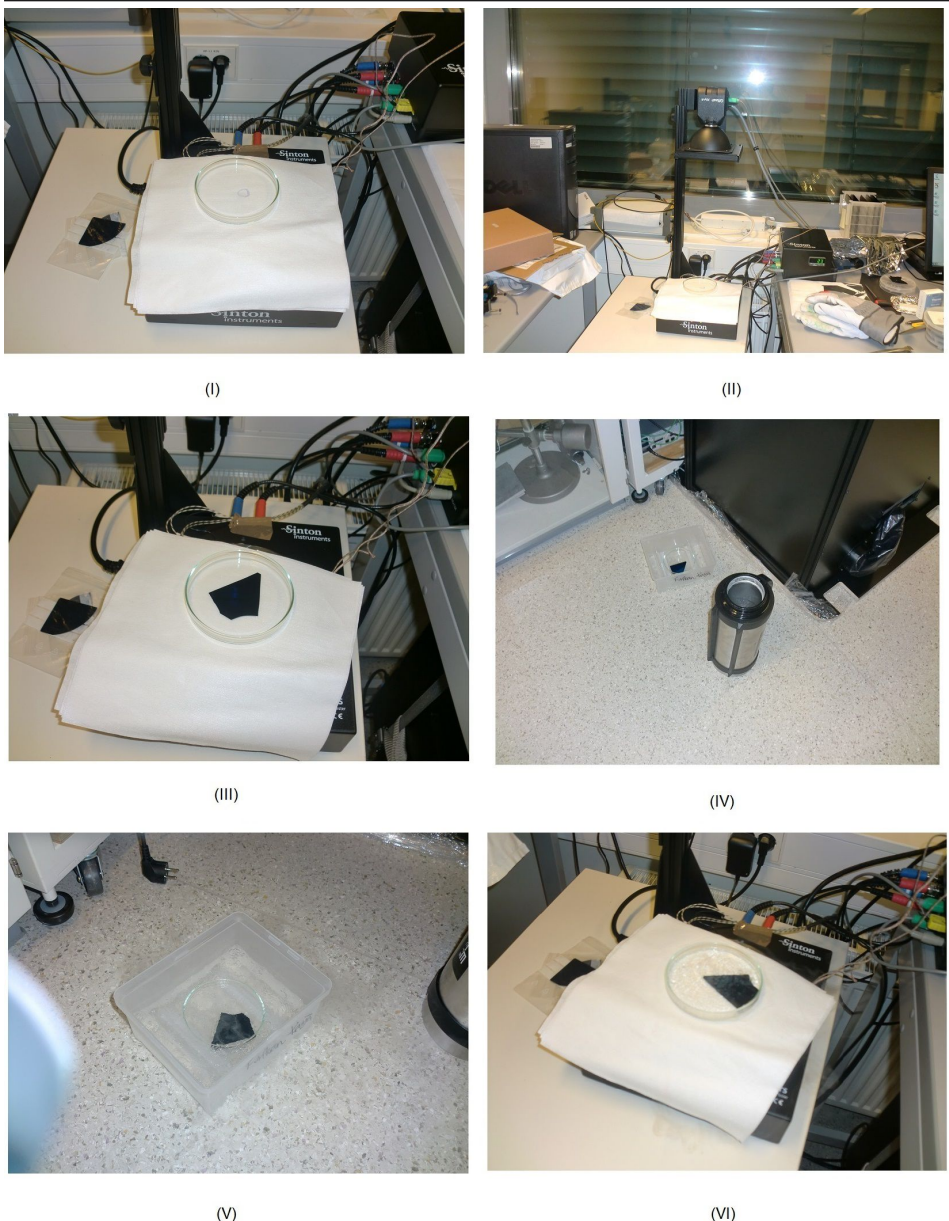


Figure 4.4: Picture montage of the entire process from calibration to measuring under CT conditions: (I) shows the setup with a circle that indicates sensors location. (II) the same setup from afar. (III) the calibration with the reference wafer. (IV) equipment used to transfer the LN₂ and the container for freezing the temperature. (V) Pyrex petridish with wafer and LN₂. (VI) Pyrex petridish placed on the WCT-120

values and compare it with "air"-values, or in our case: 5 wipes. Wipes are necessary for the protection of the vital machinery. The sensor's position is clearly indicated by the drawing of the circle. Calibration follows a least-squares fit curve:

$$F = A(V - C)^2 + B(V - C)^2 \quad (4.17)$$

where A, B and C are coefficients from the quadratic fit of the data based on measuring voltages of air and reference wafers. The practical understanding of calibration is that it shows the wafer voltage minus air voltage, which in the measurements stage includes wipes and petri dish.

Another complicating factor is to have a holder that could contain the thermal expansion when LN2 is inserted to decrease the temperature. After thorough research and conversations with experienced researchers, a petri dish made of borosilicate glass (or Pyrex as it is also occasionally named) was used. Borosilicate has a low thermal expansion coefficient at roughly 3×10^{-6} compared to between 6 and 9×10^{-6} for more ordinary glass.[28] It has high shock resistance and is capable of withstanding extreme temperatures in both ranges of the spectrum for long periods.

It quickly also became clear that due to the close proximity to other expensive equipment that the actual cool down had to happen a bit apart from the QssPC-instrument. So a disposable box made of plastic to do the experiment in and a thermos to carry the LN2 was also required.

4.5 PL Imaging for lifetime measurements

Photoluminescence imaging is a technique used to characterize crystalline silicon wafers. The method is contactless, non-destructive and gives high spatial resolution.[7]

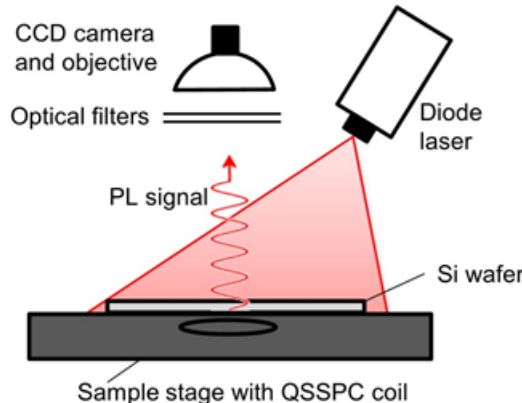


Figure 4.5: Illustration of the PL imaging equipment. A defocused diode laser is used to inject carriers homogeneously over the wafer. The emitted PL light is then detected by a Si CCD camera, with a resolution down to $23 \mu\text{m}$.[7]

In general, photoluminescence is the spontaneous emission of light from a material under illumination.[24] This occurs because of radiative recombination, where an electron from the conduction band recombines with a hole from the valence band and thereby releasing all the energy as a photon, and excess carriers are generated optically. The PL emission rate, Φ_{PL} , is therefore given as:

$$\Phi_{PL} = B_{rad}(np - n_i^2) \quad (4.18)$$

For a doped p-type material, two values are inferred, $p = N_a + \Delta n$ and $n = \Delta n$. With the relation of the intensity being:

$$I_{PL} = cB_{rad} * n * p \quad (4.19)$$

where the c is an instrument and sample specific constant describing the fraction of the emitted light which is detected by the camera.[7] For mathematical convenience the c is turned in to $c' = c * B_{rad}$ and with p and c given as in the paragraph above, the entire expression becomes:

$$I_{PL} = c'(N_a + \Delta n) \Delta n \quad (4.20)$$

From this an expression for the effective lifetime can be deducted. The effective lifetime's relation is:

$$\tau_{eff} = \frac{\Delta n}{\frac{\phi(1-R)}{W}} \quad (4.21)$$

with the newly introduced term, ϕ , being electron flux at the excitation source. After combining (4.20) and (4.21), the expression for effective lifetime is given by:

$$\tau_{eff} = \frac{\sqrt{\frac{I_{PL}}{c'}}}{\frac{\phi(1-R)}{W}} \quad (4.22)$$

Equation (4.22) clearly shows the relationship between the intensity from the PL and the effective lifetime. The domain for intensity is $5000 < I < 50000$.

The working principle for the PL system is as following: a defocused diode laser is used to inject carriers homogeneously over the wafer. The emitted PL is then detected by a CCD camera based on Si, with a resolution down to $23 \mu m$.[7]

4.6 PL measurement stage

Many of the arguments for creating the measurement stage in section 4.4 are still valid for PL. In fact even more so due to the much higher cost of the tools used for PL-I. When the PL is used, the sample is inserted into a closed chamber with a sophisticated laser and CCD camera in close proximity. LN2 in the same chamber could have adverse effect on these sensitive components.

Therefore an isopore-box with a metal sample holder that goes down into the box where the reservoir of the LN2 is meant to be. A requirement here is that the metal has very good

thermal conductivity. The two metals with the best thermal conductivity are silver and copper. In the measurement stage Aluminum is used. This is because with a thermal conductivity of $205 \frac{W}{mK}$ and other properties like strength and weight, it becomes ideal for this task. Silver and copper have thermal conductivities at 406 and $385 \frac{W}{mK}$ respectively.[29] But weigh much more and do not have the tensile properties of the Aluminum. The Al-rod extends from the bottom of the box, where it gets into contact with the LN2 and up to the top of the isopore-box, where it has the form of a rectangular sample holder. This part has been polished down in order to keep a uniformly, flat surface. A flat surface is required for getting good measurements with both the camera and avoiding unwanted effects on the wafer-sample when the laser in the PL-tool is incident on it.

With regard to the isopore-box, a material like isopore was chosen because it has high thermal isolation. It is also easy to mold, so that a cavity can be obtained. The cavity can function as a reservoir for the LN2. The box has the shape of a cube, with the dimensions 23cm * 23cm * 23cm. The walls of the box also have to be thick enough to withhold the extreme cold when temperature goes down to CT.

A picture montage presented on figure (4.6) shows all aspects of the measurement stage and how the experiment occurred with the measurement stage put into action.

4.7 The samples

For the lifetime measurements 6 samples were used. A standard Si-wafer was deposited by oxides and nitrides through a PECVD process. The passivation layer was deposited on both sides of the wafer. All the parameters can be found in table 4.1. Also indicated is a sample name given to distinguish the samples from each other.

Table 4.1: Table over the samples with sample name, passivation layer and PECVD parameters

Sample name	Passivation layer and refraction index	Deposition time
1	SiN_x	
2	SiN_x ($n = 1.9$, deposited with $\text{SiH}_4 = 10 \text{ sccm}$)	7 min (100 nm)
3	SiN_x ($n = 1.8$, deposited with $\text{SiH}_4 = 7 \text{ sccm}$)	7 min (100 nm)
4	SiN_x ($n = 1.9$, deposited with $\text{SiH}_4 = 7 \text{ sccm}$)	5 min 15 s (thin film)
5	10 nm of SiO_xN_y capped with 80 nm SiN_x ($n = 2.04$, deposited with $\text{SiH}_4 = 20 \text{ sccm}$)	4 min 50 s
6	10 nm of SiO_xN_y capped with 80 nm SiN_x ($n = 1.9$, deposited with $\text{SiH}_4 = 10 \text{ sccm}$)	4 min 50 s

Sample 1 is a generic SiN_x passivated Si-wafer with high resistivity. The samples 2-4 are deposited with a nitride layer with different deposition time and refraction indexes. Sample 5 and 6 have oxynitrides on them and oxynitrides are amorphous films consisting of Si, O, N and H. They have the same PECVD deposition time, but different refraction index and sccm.

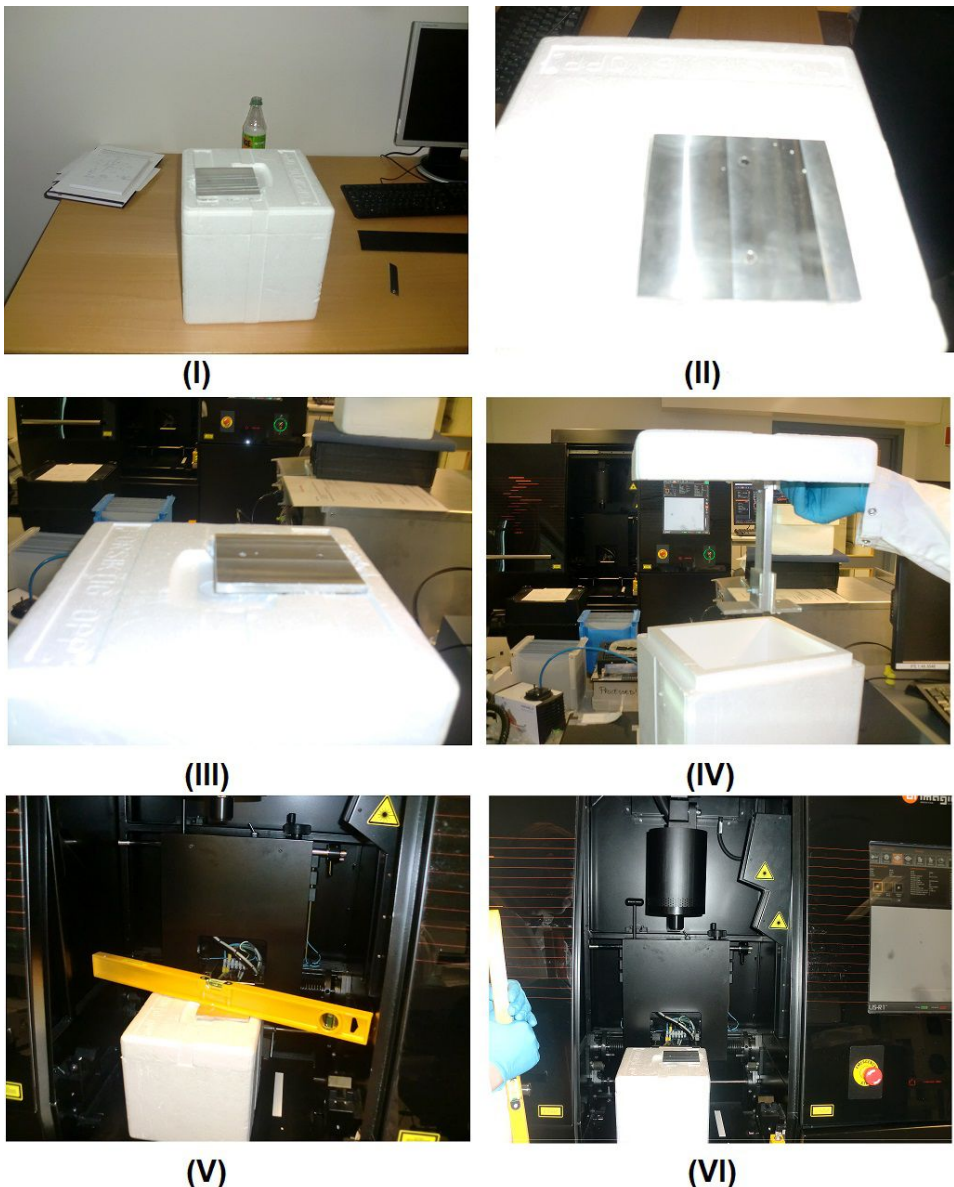


Figure 4.6: Picture montage of the PL-I measurement stage, from free standing to inserted in the PL equipment. (I) The isopore-box free standing. (II) The polished sample holder on top of the box. (III) The same sample holder viewed from the side. (IV) Cover of the box lifted up high in order to see how the Al-rod goes down to the bottom of the box. (V) A leveller is used to correct the upper position of the box, for more info referred to the experiment part. (VI) The box inserted into the PL equipment and both laser (with the danger signs attached to it on the right) and CCD camera (straight above the box) can be seen in this picture

All the samples have very high resistivity at $10\ 000\ \Omega * \text{cm}$. Wafer thickness is 0.0525 cm and the samples are p-type. In the PL figures some of them have different forms. This is because they were cut with a laser at IFE and an uniform form could not be produced.

Chapter 5

Recombination experiments and results

The chapter is built up so that it first explains the recombination experiments, before it evaluates the results achieved from the experiment.

5.1 The QssPC experiment

In section 4.5 an explanation of the new measurement stage has been given with figure 4.4 functioning as the backbone of illustrating the process. Several changes were done in the experiment compared to ordinary QssPC experiments. New calibration constants had to be found and the effect of temperature on the sensor coil had to investigated as well. A description of the procedure is given below.

1. The setup was as given in (I) on figure 4.4 with 5 wipes on the coil and petridish placed on them.
2. Wafer should be taped to the petridish with a standard laboratory tape. This is done because the LN2 is boiling and moves the wafer in the petri dish. For stable and correct measurements a tape is mandatory. However the tape could be replaced by a labpartner or weights that holds the wafer down forcefully.
3. Calibration constants for A, B and C (air voltage) in equation 4.15 were found and put in the excel-file used for measurements.
4. Petridish of borosilicate with the sample in was placed in an external holder made out of a material that also can withstand extreme temperatures (as seen in (IV) on figure 4.4)

5. LN₂ is poured on the petridish from the container for a small period. The temperature cools down very quickly and no long waiting period is needed. A thermometer was used to monitor the temperature.
6. A plier is used to move the petridish to the QssPC tool.
7. Measurements are done with a 20 seconds interval. The entire time domain varies between 10 and 15 minutes based on when it reaches the RT lifetime.
8. The mode used on the QssPC is the transient mode due to the lifetime values being above 200 μ s and it removes the need for calculation of the generation rate.

5.2 QssPC results and discussion

5.2.1 Coil and temperature influence

The coil was found to have the same lifetime values before and after cryogenic cooling. This means that its function was not affected by the cooling and that the calibration constants found during RT, could be used in CT conditions.

5.2.2 Sample lifetime measurements

Sample 1 is a generic SiN_x passivated sample used mostly as a test-sample in laboratory experiments. Despite that, it is useful for comparative matters in relation to the other samples. It could also be used to explain the general trends in the plot of the measurements.

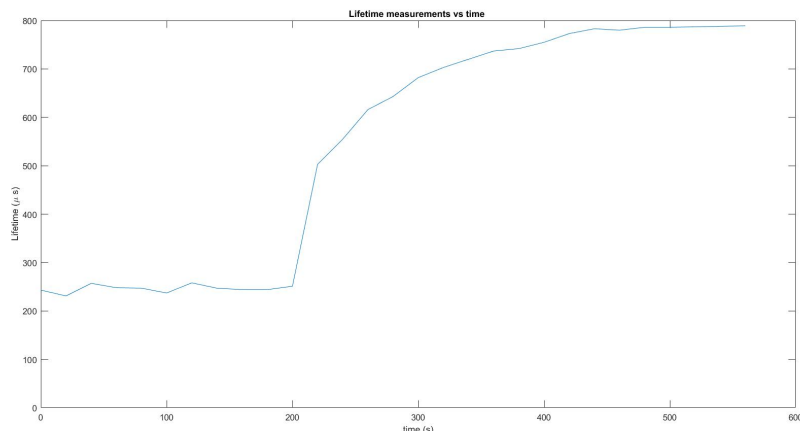


Figure 5.1: Schematic of Sample 1 lifetime measurement vs time

Figure 5.1 shows a plot of the lifetime vs time. From the figure several tendencies can be seen. The first one is the period up to 200 second. During the experiment, it should be noted that, this is the time period where LN₂ is still present in petri dish. At around the 200 second mark the LN₂ evaporates. On the plot, this gives a major jump in values to close proximity to the values found at RT. The tendency in the latter part of the plot shows a convergence toward the lifetime values found at RT as the temperature actual increases to RT.

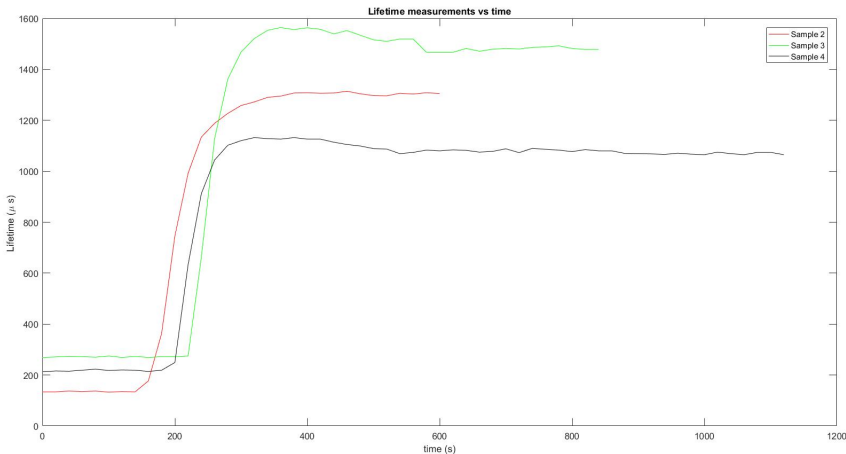


Figure 5.2: Schematic of SiN_x passivated samples lifetime measurements vs time

On the schematic of sample 2 with n = 1.9 and 10 sccm passivation, the same tendencies from the first sample can be seen again. A constant lifetime while the measurement stage containing LN₂ is seen at the interval between 0 and 140 seconds with lifetime measurement values at approximately 135 μ s. An exponential-like jump is done in the period of 180-240 seconds, with lifetime values of 363.54, 745.94, 992.70 and 1134.18 μ s. From that point on it converges to RT lifetime of 1300 μ s.

Sample 3 (green on figure 5.2) had n = 1.8 and 7 sccm passivation layer of SiN_x. It had a linearity at the measurement values of 270 μ s at CT. A jump was made at 240 s to 260 s to 1127 μ s in lifetime before a convergence is seen to RT. The lifetime at CT is roughly twice the one seen in Sample 2. Reason for that is probably the difference in refractive index and sccm. A further proof of that can be seen in the next sample on the schematic.

It also had a SiN_x layer on both sides with n = 1.9 and 7 sccm. The film is thinner than the two previous samples, but has the same refractive index as the first one and same sccm as the second one. Linearity occurs at around 220 μ s and a jump in lifetime happens at 220 seconds to 240 seconds, before a convergence to roomtemperature. The CT lifetime values are quantitatively between the middle value of the two first samples.

From the paragraph above some preliminary conclusions can be made: both decreasing the refractive index and decreasing the PECVD sccm will increase the lifetime of a Si-sample passivated by SiN_x . But more research is needed to make a final conclusion. Several tests were done on each of the samples and they all gave the same values, with the same plot trajectories.

The two final samples are both oxynitrides rather than pure nitrides. But a major dif-

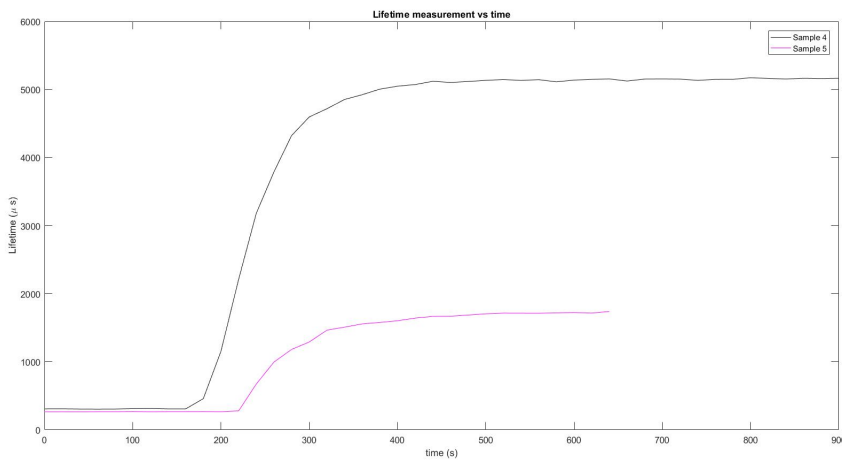


Figure 5.3: Schematic of oxynitride passivated samples lifetime measurements vs time

ference between them is the refractive index (higher for Sample 5) and PECVD deposition (also higher for Sample 5). Figure (5.3) shows that the RT lifetime is considerably higher for Sample 5 compared to the other samples. However, the lifetime measurements at CT do not reflect that. Although they are higher in value, this difference is only marginal compared to the ones in RT. The tendency shown with SiN_x regarding decreasing the n and sccm to acquire higher lifetime is not seen here. This could be due to the composition that includes oxygen in addition to nitrides.

The exponential jump when LN2 evaporates also takes longer time. It happens through a period of 140 seconds. But also here, the tendency with a linearity while under CT, followed by exponential-like jump when LN2 evaporates to the convergence to RT is seen. Linearity is seen at around $308 \mu\text{s}$.

Sample 6 was also passivated with oxynitride, but with different parameters than Sample 5. It had a considerably lower refractive index at $n = 1.9$ and lower sccm. Lower lifetime values were seen at RT, but the values at CT were not that different since the linearity occurred at $268 \mu\text{s}$. The exponential slope happened at 240 s , before the now usual convergence.

Overall there are major differences between oxynitride passivation and pure nitride passivation. The plot trajectories that indicate their properties are the same in tendency, but the values are different. This is expected since they are produced due to that fact. But the impact refractive index's and PECVD sccm has on the Si-wafer is starkly different.

One interesting phenomena worth pointing out was seen in Sample 3 and 4: the lifetime increased to above the values for RT by a big margin ($150\ \mu\text{s}$ for sample 4) and then decreased to the values for RT. This means that a recombination decrease manifested itself. But it happened at temperatures at roughly -10 degrees C to +10 degrees C rather than the assumed 77 K. Several retrials of the sample showed the same.

Sample number	Temperature	Lifetime (μs)
1	RT	650.84
1	CT	201.27
2	RT	1246.48
2	CT	138.49
3	RT	1449.93
3	CT	267.63
4	RT	1074.61
4	CT	216.85
5	RT	5165.53
5	CT	306.29
6	RT	1739.95
6	CT	266.31

Table 5.1: Table shows the sample numbers, temperature and lifetimes at respectively RT and CT

5.2.3 Explaining the lifetime values

In providing an explanation for why the lifetime values are how they are at CT, a reference is given to the literature from S. Rein.[26] Most of the following paragraphs in the subsection are based on those theories. As seen on the schematics in the figures from this section, the recombination actually increases. One of the objectives for improvement of photodiodes was to decrease recombination by a factor of an logarithmic order of 1 to 2. The following section explains why the opposite is the case for the samples.

From the measurements in chapter 3 on the PQED photodiodes, it was seen that the photodiode significantly improved its performance at CT. Deduced from that was that a similar tendency should be seen in the lifetime values because of the implied decrease in recombination. Lifetime results done on the passivated wafers did not concur with that theory. To be able to explain this phenomena, two terms are re-introduced: shallow and deep defects. The difference between deep and shallow-level defects is the amount of energy needed to remove an electron or hole from the defect to the valence or conduction band.

With a foundation in equation (4.7) and (4.8); τ_{n0} and τ_{p0} has a weakly negative temperature-coefficient ($T^{-1/2}$). This leads to for deep defects, that n_1 and p_1 becomes very small and a lifetime time that goes up with decreasing temperature is seen. If shallow defects dominate, the exponential T-dependency in n_1 and p_1 is the strongest T-dependency, and a decreasing lifetime proportionally follows a decreasing temperature. It seems the last phenomena is seen with the samples used in this project.

Two more terms must be introduced to explain the phenomena further; the relative defect parameters, k and E_t . k is a symmetry factor and is defined as the extent of the capture asymmetry and is a characteristic feature of a defect state. k is given by:

$$k = \frac{\tau_{p0}}{\tau_{n0}} \quad (5.1)$$

Equation (5.1) depends only on the defect structure and is like the energy level, E_t , a relative defect parameter. By replacing τ_{p0} with k , the equation (4.6) becomes with low-level injection and p-type Si:

$$\tau_{SRH} = \tau_{n0} \left[\left(1 + \frac{p_1}{p_0} \right) + k \left(\frac{n_1}{n_0} \right) \right] \quad (5.2)$$

The parameters E_t and k have a crucial influence on the SRH lifetime. The two terms and lifetime are connected through:

Position of E_t in band	Magnitude of relative densities	R. activity of the defect
Deep level defect close to mid-gap: $E_t = E_{gap}/2$	$p_1, n_1 \ll p_0$	$\tau_{SRH}/\tau_{n0} = 1$
Shallow defect level close to VB: $E_t - > E_V$ close to CB: $E_t - > E_C$	$n_1 \ll p_0 \ll p_1$ $p_1 \ll p_0 \ll n_1$	$\tau_{SRH}/\tau_{n0} = p_1/p_0$ $\tau_{SRH}/\tau_{n0} = k(\frac{n_1}{p_0})$

Table 5.2: Table shows the relationship between E_t , k and lifetime. R. in column is recombination

Table 5.2 shows that deep defects with energy levels close to mid-gap are most effective for recombination, independent of doping concentration. Shallow defects, on the other hand, with energy levels many kT from mid-gap contributes to the recombination at high doping concentration.

By putting $k = 1$ (meaning symmetry), defects with the same energy-distance to the mid-gap have the same recombination rate. However, by putting $k \neq 1$, a different scenario unfolds. Then the recombination increases with a lower symmetry factor k .

Equation (5.2) becomes under low-level injection:

$$\frac{\tau_{SRH}}{\tau_{n0}} = 1 + k \left(\frac{n_1}{p_0} \right) \quad (5.3)$$

For a deep level defect, the ratio $\frac{n_1}{p_0}$ has no influence on the τ_{SRH} . This is the case for both temperature and doping concentration variations. For a shallow level a variation of the ratio leads to a change. Decreasing doping and increasing temperature leads to an increase in lifetime. From this a confirmation of the extent of shallow level defects is obvious due to lifetime lowering at CT.

In the conduction band the recombination is limited by hole capture and a k increase corresponds to a decrease in the relative capture cross-section for holes. That means that the recombination activity of the defects decreases with increasing k, and this leads to lower temperatures for the Arrhenius increase.

The Arrhenius equation concerns the temperature dependence of reaction rates. A standard rule taken from Rein, is that the shallower the energy level of a defect, the lower the slope of the Arrhenius increase of τ_{SRH} and the lower the temperature of its onset. A direct consequence of this rule is that reduction in doping gives lower recombination activity and an increase in k. From that, the onset of the Arrhenius increase can be moved to lower temperatures, basically meaning higher lifetimes with lower doping concentration. The PQED has a doping concentration of 10^{12} , while the wafers measured have a doping concentration, from the resistivity, at roughly the same. Doping could be higher in the wafers because the PQED has an inversion layer to compensate for lower doping.

The theories above could give some pointers to why the lifetimes are as they are. But more measurements are necessary to provide complete confirmation. However, based on theories with a foundation in simulation, it was assumed that the recombination would automatically decrease for all passivated Si-wafers at 77 K. For the investigated passivation layers, it has proven not to be the case.

5.2.4 Mobility approximation

The Dannhauser/Krause model was the mobility model used in the transient QssPC measurements. In the Excel-software a Calc-function is used to obtain the mobility values. The model is a temperature-independent model. The following paragraphs will attempt to create an approximation for the mobility.

Relationship between resistivity, ρ , and conductivity, σ , is given by $\frac{1}{\rho} = \sigma$. Furthermore, the expression for conductivity as a function of mobility is:

$$\Delta \sigma(t) = qn\mu_n + qp\mu_p = q(\mu_n + \mu_p) \Delta n \quad (5.4)$$

With $n = p = \Delta n$, the equation (5.2) can be rewritten to:

$$\Delta n(t) = \frac{\Delta \sigma}{q(\mu_n + \mu_p)} \quad (5.5)$$

The transient function does not take into account generation, so the transient lifetime is given by:

$$\tau_{transient}(t) = \frac{-\Delta n(t)}{\frac{d\Delta n(t)}{dt}} = \frac{\frac{-\Delta\sigma(t)}{q(\mu_n + \mu_p)}}{\frac{d}{dt} \left[\frac{\Delta\sigma(t)}{q(\mu_n + \mu_p)} \right]} \quad (5.6)$$

Assuming that μ_n and μ_p are independent of t and Δn , the expression becomes:

$$\tau_{transient}(t) = \frac{\frac{-1}{q(\mu_n + \mu_p)}}{\frac{1}{q(\mu_n + \mu_p)}} \frac{\Delta\sigma(t)}{\frac{d\Delta\sigma(t)}{dt}} \quad (5.7)$$

leading to the final expression of:

$$\frac{-\Delta\sigma(t)}{\frac{d\Delta\sigma(t)}{dt}} \quad (5.8)$$

The approximation in equation (5.8) suggests that in the transient mode, lifetime is independent of mobility. This makes it potentially a good approximation for the Dannhauser/Krause model.

5.2.5 High temperature measurement experiment for comparison

Lifetime measurements were done at HT in order to provide comparison with RT and CT measurements. No adjustment for mobility is necessary since this is already done in the QssPC software.

The experiment:

1. The heater connected to the QssPC tools is heated up to 375 K. A value slightly above 373 K is needed for the measurement.
2. Mode called temperature scan on the QssPC software is turned on. All tasks required on the computer should be done.
3. Pick a measurement interval of 373 K to 303 K. Tune the desired end temperature on the heater to 273 K.
4. Transient mode on the QssPC was chosen.
5. A measuring step of 5 K is used. This means that the coil measures for each 5 K and a flash should be seen at these specific point: 373 K, 368 K, 363 K...303K. In total 15 measurements were done.
6. Use the "sample data" and "redo plot" functions in the excel-file. A automatic plot-file is created if the entire interval from step 3 is measured.

Two results obtained by the HT experiment is given in this text. First one is of Sample 2 and the second is of Sample 5. Sample 2 has a nitride passivation layer and Sample 5

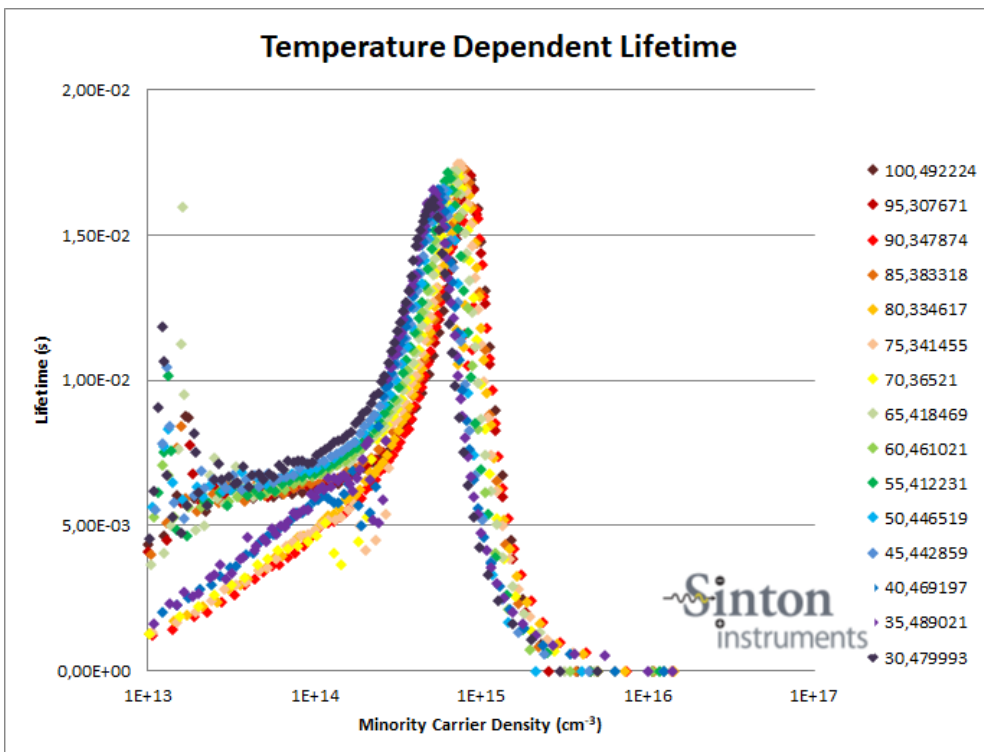


Figure 5.4: Schematic of effective lifetime vs minority carrier density for different temperatures. The measured sample is Sample 2.

has a oxynitride passivation layer. Based on the different temperature plots in figure 5.4, the tendency of decreasing lifetime proportional to the decreasing temperature can be confirmed. That specific phenomena can be seen from HT to RT to CT. And that validates that the CT values were not due to an aberration of some sort.

The second result was from the Sample 5. This sample had much higher lifetime values than the others at RT, while the difference was only marginal at CT. Therefore a comparison of the lifetime evolution of Sample 2 and Sample 5 could prove interesting.

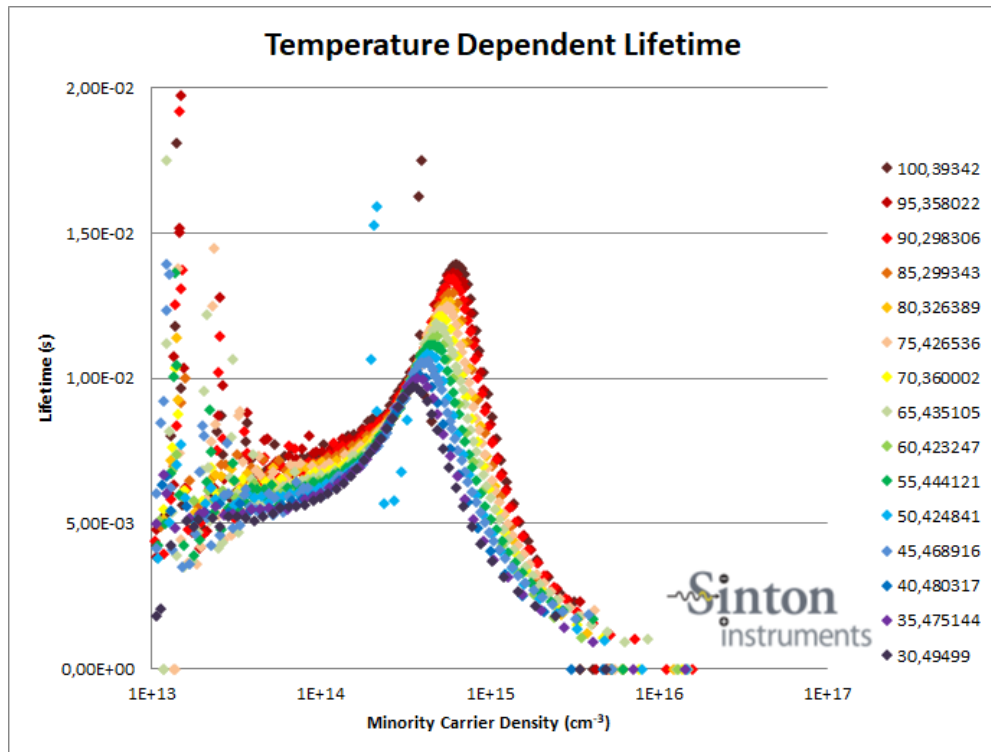


Figure 5.5: Schematic of effective lifetime vs minority carrier density for different temperatures. The measured sample is Sample 5.

The slopes of the two samples in figure 5.4 and 5.5 are not the same. However, the tendency with the decreasing lifetime from HT to RT to CT is the same. One interesting point worth noticing with the two lifetimes is that the maximum lifetime value of Sample 5 is not higher than the one for Sample 2. This was the case at RT.

Last schematic in this section is a comparison of the lifetime vs minority carrier density for HT, RT and CT conditions.

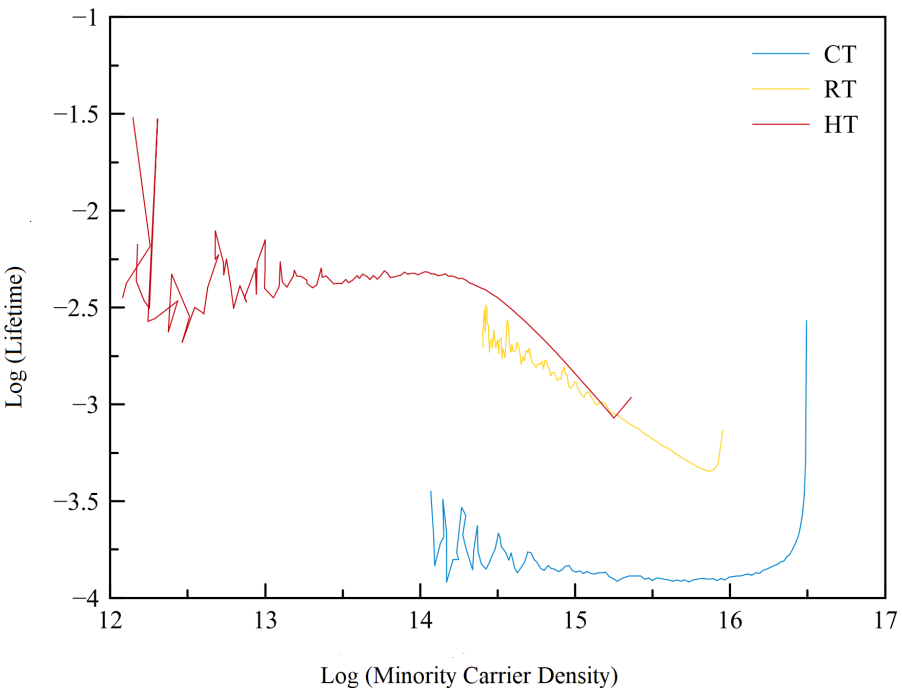


Figure 5.6: Schematic of log/log scale plot of lifetime measurement vs minority carrier density for Sample 2 for HT, RT and CT. Lifetime is given in μs and minority carrier density in cm^{-3}

The schematic from figure 5.6 are plotted in a new way compared to the other plots in this project. Rather than having temperature as a variable, the new variables are lifetime and minority carrier density. In this schematic the temperature is fixed at 373 K (red line), 303 K (yellow line) and 77 K (blue line).

On figure 5.6, some similarities between the plots of CT and RT can be seen. They both initiate at a later minority carrier density and their lifetimes fluctuate less in their plots. The plot of RT seems to be a middle point in shape between HT and CT. And it should be pointed out that the tendency seen in lifetimes previously is roughly the same, with a big exception at minority carrier density value of 16.5 in logarithmic scale. At that point the lifetime for CT is considerably higher than for both RT and HT. But this is most likely to be an artefact.

5.2.6 Evaluation of the measurement stage

The measurement stage for QssOC was fairly simplistic and built with parts found in every laboratory. In an evaluation several aspects of the experiment has to be considered. The criteria are formed as questions and thereafter answered:

Did the experiment succeed or not?

The intention with the experiment was to obtain Si-wafer lifetimes at CT conditions. Nothing damaging happened with the equipment due to use of LN2. Based on that the criteria the experiment was satisfying.

Can the experiment be easily replicated?

Most of the material used to create the measurement stage can be found in most laboratories. The steps necessary to do the experiment are also not very complicated. The experiment should be easily replicated.

Was the cryogenic temperature of 77 K reached?

The temperature was reached without problem and as long as the LN2 was in the petridish, the CT uphold itself in order for the measurements to done. When the LN2 evaporated the temperature increased dramatically.

Were the results satisfactory?

The results obtained are interesting. But a recombination decrease with a logarithmic factor of one to two order of magnitudes was not seen. This would imply a likewise increase of lifetime. The reason for this is most likely due to the material composition and not due to the failure of the experiment.

Were the security precautions followed?

LN2 is hazardous and can cause rapid suffocation and severe frostbite. The first one due inhalation and second one due to in contact with the human skin.[30] This requires a person working with LN2 to not work in a closed room or have the LN2 in a closed volume. The frostbite can happen as a result of contact and a labcoat that covers all of the body with thick gloves on is mandatory to work with LN2. All of these security precautions were followed.

Having considered all the factors above, the QssPC measurement stage can be considered to be a success.

5.3 PL experiment

Measurement stage for PL has already been elaborated on in section 4.6. Figure 4.6 should be referred to. The experimental procedure follows next.

1. Mandatory protective equipment for work under CT conditions like gloves, labcoat and goggles should be put on.

2. The measurement stage specially designed for PL is placed on the ground or an another space where contamination is allowed.
3. LN2 is introduced into the isopore-box. Due to the volume of the box, several instant refills might be necessary in order to create a reservoir.
4. A holder for the isopore-box is placed instead of the coil of the QssPC part of the equipment. The box should be leveled so that the sampleholder at the top of the box is in line with the detectionlimit of the laser and CCD camera. This means that the coil should be pulled down and a plate with the correct dimensions be placed its place.
5. The filled box should be lifted carefully to the holder in the PL. If in doubt about the strength of the box, an another plastic box, where the isopore-box can be placed in, can be used.
6. Put wafer on the sample-holder made of metal.
7. Wait until the metal gets frozen. The same condition can be said about the wafer. Step 7 might take upward to 20 minutes.
8. Measure the lifetime of the sample by creating own parameters in the software of the PL.
9. Carry the PL box outdoors and empty it of the LN2. Alternatively leave the box open in a safe space in order for the LN2 to evaporate (but it cannot be done unsupervised in a closed room). This step requires all safety procedures like gloves and other protective measures to be followed.

5.4 PL results and discussion

When analyzing the PL results, some explanations on how to evaluate the images is necessary. On an image, the colour contour is not uniform across the Si-wafer. Some parts are red, some are yellow like, while others look to be white. Based on the intensity-chart to the right of the image and equation (4.22), it is understood that the white area represents high lifetime, while the red area indicated where the lifetime is lowest.

The basic outline in representing the images are RT images of the Samples 2-6 to the left and the RT images of the samples to the right. All of the images are uncalibrated, but it should be enough to evaluate the lifetimes.

On the intensity bars at the right on figure 5.7, and while remembering equation (4.22), it is given that the light area is high lifetime and dark area is low lifetime. All of the Si-wafers are passivated by nitride and it is clearly seen that on all the wafers that the CT measured wafers have low lifetime uniformly spread through the sample. Compared to the wafers measured under RT conditions, there is a clear difference. The RT wafers are mostly light with high lifetime, but dark in some areas. Dark areas are probably due to impurities from

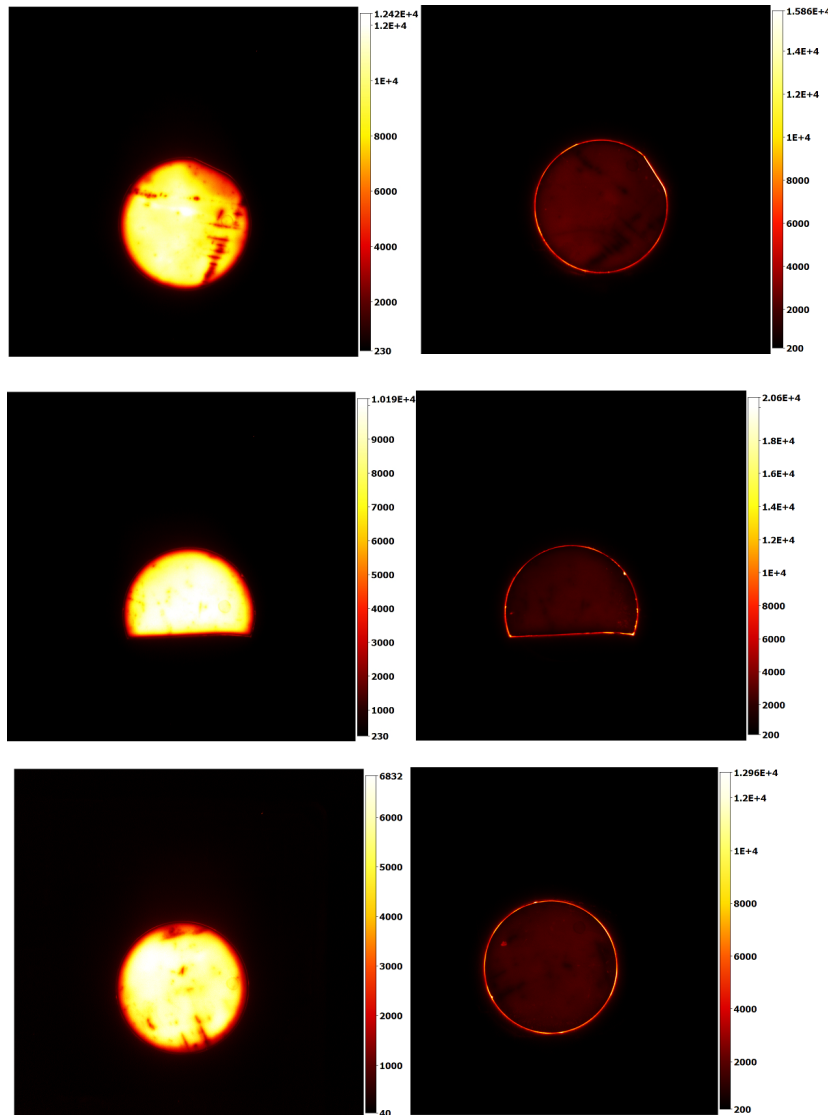


Figure 5.7: Images that shows the results obtained by PL-I for the SiN_x passivated layers. The upper image depicts Sample 2, the mid-tier image depicts Sample 3, while the last image depicts Sample 4. On all the rows, RT to the left and CT to the right

the PECVD process when creating the wafer.

Figure 5.8 shows PL-I values for the oxynitride samples. The tendency seen for the purely nitride passivated samples is seen again. Lifetime is significantly decreased at CT compared to RT.

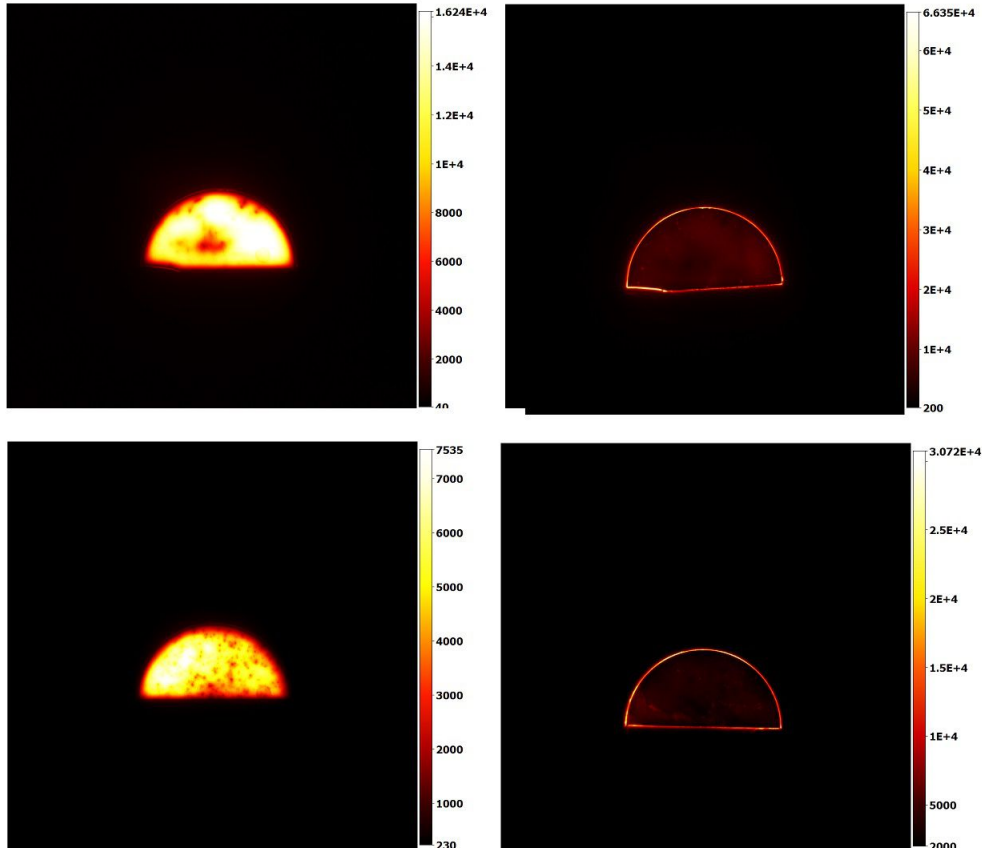


Figure 5.8: Images that show the results obtained by PL-I for the oxynitride passivated layer. The upper image depicts Sample 5 and the lower image depicts the Sample 6

PL-I results confirm the results presented from the QssPC experiments. The lifetime at CT significantly decreases compared to the lifetime results from RT. One difference between the two measurement methods is seen on figures 5.7 and 5.8: the edges of the wafers on the PL images is much higher than the rest of the wafer. Comparing it with QssPC shows that QssPC gives the opposite.

Reason for the difference could be that in the QssPC experiment, the sample is completely submersed in LN₂. In the PL experiment, the thickness of the wafer leads to less

temperature-effect on the edges. There is a distance between the wafer edges and the sample holder. The distance is given by the wafer thickness.

5.4.1 Evaluation of the measurement stage

The criteria for evaluating the QssPC stage is applicable to the PL stage as well. Main differences between the two measuring methods is the more complicated equipment of the PL-I and the considerably higher price of the PL-I.

Did the experiment succeed or not?

This measurement stage was more complicating to evaluate compared to the one for QssPC. Al was used as the metal to conduct the cold up to the sample holder from the reservoir. Other metals like silver and copper would have done that job better, but are either more expensive, brittle or just heavier. Based on Rein the measurements obtained at 150 K do not deviate much from the ones obtained at 77 K.[26] And the results obtained showed enough of a tendency to be considered a success. The other factor regarding the preservation of the equipment also went without problems since the equipment was not affected at all.

Can the experiment be easily replicated?

If the necessary components to create the isopore-box with a metal-rod to lead the cold can be obtained, then the experiment can be replicated without problems.

Was the cryogenic temperature of 77 K reached?

No. However the results from 150 K and below to 77 K obtained from a PL-I are the same. From semiconductor physics it is theorized that at intermediate temperatures (RT) the carrier density is equal to doping, while at high temperatures (HT) it increases, before it decreases at CT due to incomplete ionization of the dopants.[26] This can also be seen in figure 5.6. Therefore the obtained temperature of 173 K with an unreliable multimeter is sufficient for the task.

Were the results satisfactory?

The obtained results from both RT and CT show a major decreasing lifetime for CT compared to RT. This is in agreement with the lifetime results for the QssPC measurement stage. Inferred from that, is that the results are satisfying.

Were the security precautions followed?

The by now standard precautions like protective wear was followed. But the PL-I measurement stage was extra dangerous compared to the QssPC measurement stage. This is because the person doing the experiment has to carry the isopore-box to the equipment. Spill-danger is rather hight when this procedure is done. The box has to be carried when

the LN2 has to be spilt outside also. One could have the box in an open space so that the LN2 evaporates, but this will take many hours and in that amount of time accidents could occur. Despite all the potential risks, the novel exmperiment went without accidents.

The filled-out evaluation form strongly indicates a fully functional measurement stage and despite the optimal temperature not reached, the actual temperature reached was sufficient for the experiment and other likewise projects. An improvement could be to change the metal the sampleholder is made of. Silver or copper could both potentially be used. Making the sampleholder at the top of the box (see figure 4.6) thinner could also be an option. However, the final conclusion with regards must be that it was a successful measurement stage.

Chapter

6

Overview of the results

As a result of the large flux of results presented, it might seem difficult for the reader to comprehend all the results obtained by the experiments. Therefore a overview of them is given in this chapter.

Measurement stage for QssPC: Temperature for the wafer went down to 77 K and the measurements corresponds with the assumed values. None of the material and equipment used during the experiment was destroyed. If correct safety measures, like thick protective gloves, labcoat (with a sweater beneath) that covers the entire body and goggles are used, the person doing the experiment is safe as well. Conclusion drawn is that the measurement stage for QssPC is a success!

Measurement stage for PL: Only applicable for PL-I and the QssPC part of PL is not possible to do. However, that was not the intention either. The temperature for the wafer went down to 173 K. Experimentally this was enough to confirm whether lifetime decreased or increased and could be used as a comparison to the QssPC measurements. Conclusion drawn is that this measurement stage was a success as well!

Linearity for the photodiode: A comparison between the I-V curves for the SiO₂ passivated layers at RT and CT was conducted. The linearity for the measurements CT is considerably longer than the one acquired for RT curve. Major ramifications for fields like detectors and quantum computing can be foreseen from this.

Uncertainty measurements for the photodiode: Again a comparative study was done between the uncertainty for a photodiode at RT and CT. Values gained showed great promise for the future due to the low uncertainty. The uncertainty was at roughly 0.25 ppm. This is far below the desired value of 1 ppm that would give a 1:1 ratio between incident photons and externally measured photoelectrons.

Influence on sensor coil from the temperature-change: The sensor coil showed no sign of giving different lifetime due to a change of temperature. Because of this no further calibration was needed. To put it simpler: no additional calibration had to be done after the CT was reached, after an initial calibration for the measurement stage.

Decreasing lifetime values at CT: All wafer show a decrease of lifetime measurement values at CT. This decrease is by roughly a logarithmic factor of 1 for the nitride passivated wafers, while it is by a factor of 20 for the oxynitride passivated wafers. Despite showing a great difference in lifetime values at RT, this was not observed at CT.

Similar slopes for all plots, independent of passivation layer used: A plot of lifetime values vs temperature was done for all 6 samples with different passivation layers. They all showed similar slopes with a constant lifetime when LN2 still in the measurement stage, an exponential rise when LN2 evaporated and a slow convergence toward the lifetime values as the temperature slowly went toward RT.

Refractive index and its influence on lifetime: Measurements done on the SiN_x passivated layers showed that a lower refractive index and a lower value in PECVD parameters influenced the lifetime. It increased the lifetime, but needs more experimental data to confirm.

Comparison between passivation material: No oxides were present as passivation layer, but oxynitride with a combination of among other oxygen and nitrogen was used. The nitride layer with the lowest refractive index proved to be the best passivation layer. It had almost the same lifetime values at CT as the oxynitride material with RT values at over 5000 μs , despite only having a value about a quarter of it at RT. Refractive index seems to be more important than the passivation layer. In a master thesis an oxide layer will be used as a passivation layer in order to provide further comparison cases.

An explanation of the lifetime values: An explanation is provided, but needs further test for whether it upholds in the scientific limelight.

The effect of mobility on recombination at CT: An approximation has been done on the mobility used in the QssPC tool. One important takeaway is that for the transient-modus the lifetime is independent of the combined electron and hole mobility.

HT lifetime measurements: Measurements were done at HT = 373 K to provide a comparison with CT and RT conditions. These were so plotted together in a graph. HT and RT were slightly different, but had the same trajectory as a function of the minority carrier density. The CT lifetime had the opposite slope and had a peak at a much later value of density.

PL-I measurements confirms QssPC measurements: PL-I measurements showed that the lifetime of the wafers decreased with a large amount when exposed for CT conditions. This confirms the main take-away from the QssPC measurements about the decreasing lifetime values at CT.

Conclusion

Several goals for the project were outlined in section 1.1. In evaluating the project, it is natural to look at those and see whether they accomplished or not. Two measurement stages were created for use in QssPC and PL tools. Both were successfully created and tested. Despite several potential risk hazards, they were all avoided due to precautions and diligent preparation.

A potentially new standard is within reach since the uncertainty was proven to be below the values desired. However, more testing is needed in order to confirm this. One problem with having a panoply of goals is the time constraint imposed. However good planning could remedy that.

The decrease in recombination at CT from the simulations was not seen. Instead the opposite occurred. Several explanations are given in the text for why this happened. The samples need different passivation layers for the project to reach to the bottom of this conundrum. Effect of mobility on recombination was also investigated and measurements at both RT and HT were done for comparison. The tendencies seen at measurements done with the measurement stages were strengthened with higher temperature experiments.

Oxide layers were sadly not available for the project to fulfill the last aspect of the goals. Oxynitride and nitride passivation layers went through intensive testing. Several results were obtained and theories have been created for further work on that.

7.1 Possible future work

- **Making improvements in the measurement stages:** Several improvements have been suggested in the text already. These are for example changing the Al-rod in the PL stage with silver. Other changes could be found when more testing has been done on different passivation layer materials.

- **Linear optical quantum computing:** is a form of quantum computation that uses photons as information carriers and mainly uses linear optical elements to process information and photon detectors to detect quantum information.

Therefore it is very useful to reduce the uncertainty to 1 ppm for photodiodes and to check for how long the linearity of the photodiode continues, which it does for a longer time under CT conditions. Results from this project could lead to further breakthroughs within the nowadays largely theoretical fields of both quantum and optical computing

- **Decreasing the refractive index and PECVD sccm:** Some preliminary results from the SiN_x passivation layer indicates that this will increase the carrier lifetime and decrease recombination. An easy way to decrease the refractive index is by increasing the wavelength of the incident photon. But this is not feasible with the QssPC tool. However, it could be done with the PL laser. A more likely method to decrease the refractive index is through the composition of the passivation-wafer interface and changing the process conditions.
- **Doing so-called PL-V measurements** (as a function of the temperature) by applying voltage on the passivation layers in the lifetime measurements.
- **Testing different passivation layers:** Pure oxide layers were not tested on in this project. Future work could entail work on wafers with a different material composition to compare it with the materials in this project. ...

Bibliography

- [1] Gran, J.; Tang, C. K.; Nordsveen, M. U. *Metrologia* **2017**, *14*, 1–7.
- [2] Skauli, T. *Imaging and detection of optical and infrared radiation - Lecture notes*; Selfpublished: Kjeller, 2017; Chapter 6,8,22, pp 141–426.
- [3] Gran, J.; et al., *Metrologia* **2013**, *50*, 385–395.
- [4] Schroder, K. *Semiconductor material and device characterization*; John Wiley Sons, Inc.: Hoboken, New Jersey., 2006; Chapter 6,7,8, pp 319–521.
- [5] Black, L. *New perspectives on surface passivation: understanding the Si-Al₂O₃ interface*; Springer: Canberra, 2016; Chapter 2, pp 15–28.
- [6] UserManual, *WCT-120 Photoconductance lifetime tester - User manual*; Sinton Instruments: Boulder, CO, USA, 2013; pp 1–46.
- [7] Haug, H. *New methods for investigation of surface passivation layers for crystalline silicon solar cells*; AIT Oslo AS: Oslo, 2014; Chapter 1–6, pp 1–93.
- [8] ElectronicsTutorial PN Junction Theory. http://www.electronics-tutorials.ws/diode/diode_2.html, Accessed: 2017-11-14.
- [9] Storey, N. *Electronics: A systems approach*; Pearson Education Limited: Harlow, UK, 2013; Chapter 17, pp 309–334.
- [10] Hansen, T. *Physica Scripta* **1978**, *18*, 471–475.
- [11] Proceedings of NEWRAD 2011.
- [12] Streetman, B.; Kumar, S. *Solid state electronic devices*; Pearson Education Limited: Harlow, UK, 2016; Chapter 2, pp 54–55.
- [13] Raklev, A.; Engeland, T.; Viefers, S.; Hjorth-Jensen, M. *Compendia in FYS2140: Quantum Physics*; Akademika: Oslo, 2016; Chapter 2, pp 19–23.

BIBLIOGRAPHY

- [14] Kittel, C. *Introduction to Solid State Physics*; John Wiley & Sons, Inc: Hoboken, NJ, 2005; Chapter 8, pp 185–218.
- [15] AP Technologies *Photodiode Theory of Operation*. 2017; <https://www.aptechnologies.co.uk/support/photodiodes/photodiode-theory-of-operation>.
- [16] Gran, J. Accurate and independent spectral response scale based on silicon trap detectors and spectrally invariant detectors. Ph.D. thesis, University of Oslo.
- [17] M.Salahinejad,; F.Aflaki, *Measurement Science Review* **2007**, 7, 67–75.
- [18] Gran, J.; Kubarsepp, T.; Sildoja, M.; Manoocheri, F.; Ikonen, E.; Muller, I. *Metrologia* **2012**, 49, 130–134.
- [19] Tang, C. K.; Gran, J.; Muller, I.; Linke, U.; Werner, L. *Proceedings NUSOD 2015 2015*,
- [20] Tang, C. K.; Gran, J.; Haug, H.; Stokkan, T. S. *Proceedings NEWRAD 2017 2017*,
- [21] Geist, J.; Brida, G.; Rastello, M. L. *Metrologia* **2003**, 40, S132.
- [22] Manoocheri, F. Predictable Quantum Efficient Detector (PQED). 2013; <http://metrology.tkk.fi/orm/pqed/>.
- [23] Courtois, G.; Bruneau, B.; Sobkowicz, I. P.; Salomon, A.; i Cabarrocas, P. R. *MRS Online Proceeding Library Archive* **2013**, 1536, 1–6.
- [24] Godia, A. R. Nanoscale spatially-resolved characterization of photovoltaic devices and materials. Ph.D. thesis, Autonomous University of Barcelona.
- [25] Brechignac, C.; Houdy, P.; Lahmani, M. *Nanomaterials and nanochemistry*; Springer: Berlin Heidelberg, 2007; Chapter 1, pp 1–32.
- [26] Rein, S. *Lifetime Spectroscopy: a method of defect characterization in silicon for photovoltaic applications*; Springer: Berlin, 2005; Chapter 1,2,3, pp 5–253.
- [27] Soppe, W. J.; Devile, C.; Schiermeier, S.; J.Hong,; Kessels, W.; van de Sanden, M.; Arnoldbik, W.; Weeber, A. *ECN Solar Energy, Proceedings 17th European Photovoltaic Solar Energy Conference, Munich (2001)*. **2001**,
- [28] TheEngineeringtoolbox, Coefficients of Linear Thermal Expansion. 2017; https://www.engineeringtoolbox.com/linear-expansion-coefficients-d_95.html.
- [29] Hyperphysics Thermal Conductivity. <http://hyperphysics.phy-astr.gsu.edu/hbase/Tables/thrcn.html>, Accessed: 2017-10-22.
- [30] Refrigeration Oxygen Co. Liquid Nitrogen safety datasheet. <http://microfluidics.cnsi.ucsb.edu/msds/LN2%20r2.pdf>, Accessed: 2017-09-11.

Appendix

APPENDIX A: Processplan

In this part, the researcher has made an attempt to give a plan over the entire process: from the project paper to the master thesis.

Part one: Project before Christmas

- Acquiring theory about induced photodiodes, lifetime measurements and the passivation materials
- Familiarizing with the equipment (QssPC, PL and laser setup at JV)
- Creating a measurement stage for cryogenic temperature that protects the equipment and can last through the low temperature measurements without breaking apart
- Measurements on existing test samples
- Measurements on response to induced photodiodes as a function of temperature (at both IFE and JV)

Part two: Master thesis in the spring

- Lifetime measurements on different passivation samples as a function of temperature. Must be done on the developed measurement stage from the previous semester
- Making simulation parameter's from the measurements
- Understanding the results and comparing with the theory (basically the results we were expecting to get in the introduction and theory)
- Working on simulation at JV for low temperature

BIBLIOGRAPHY

APPENDIX B: List of software used in the thesis

Appendix B will give a walkthrough of the software used in this thesis.

Microsoft Excel: A standard spreadsheet software from Microsoft. Was used to make tables. It was the software used by producer Sinton Instruments for their QssPC tools WCT-120 as part of its software to analyze the lifetime values.

ShareLaTeX: ShareLaTeX is a compiler on the line of Microsoft Word. But has the advantage that it makes the equations and images inserted easier to use and makes the text seem more elegant compared to its competitor. Requires intermediate coding skills.

MATLAB: MATLAB is a numerical computing program. It can be used to plot functions, manipulate matrices and implement algorithms. Several of the plots in the thesis are created with MATLAB.

LabView: LabView was used to create the circuits in the JV laboratory. These circuits were later implemented. The software was also used to monitor the measurements from remote distances.

CircuitLab: This online website was used to design circuits used in this thesis.

Cogenda Genius: A simulation program used to simulate the creation of PQED and other aspects, like lifetime and passivation layers.

P1CD: P1CD is a simulation program similar to Cogenda Genius. Is used in several courses at UNIK and can be used to many things within the field of simulation. Particularly effective for work with solar cells.

MagicPlot: A software used to almost exclusively plot function. Easier to transfer tables from Excel and creates plots that sometimes might look better than those with MATLAB.